# EXPERIMENTAL MEASUREMENTS AND MODELING PREDICTION OF FLAMMABILITY LIMITS OF BINARY HYDROCARBON MIXTURES

A Thesis

by

FUMAN ZHAO

Submitted to the Office of Graduate Studies of
Texas A&M University
in partial fulfillment of the requirements for the degree of

MASTER OF SCIENCE

May 2008

Major Subject: Chemical Engineering

# EXPERIMENTAL MEASUREMENTS AND MODELING PREDICTION OF FLAMMABILITY LIMITS OF BINARY HYDROCARBON MIXTURES

A Thesis

by

FUMAN ZHAO

Submitted to the Office of Graduate Studies of
Texas A&M University
in partial fulfillment of the requirements for the degree of

MASTER OF SCIENCE

Approved by:

| | |
|---|---|
| Chair of Committee, | M. Sam Mannan |
| Committee Members, | Kenneth R. Hall |
| | Debjyoti Banerjee |
| Head of Department, | Michael V. Pishko |

May 2008

Major Subject: Chemical Engineering

# ABSTRACT

Experimental Measurements and Modeling Prediction of Flammability Limits of Binary Hydrocarbon Mixtures. (May 2008)

Fuman Zhao, B.S., University of Tianjin

M.S., Texas A&M University

Chair of Advisory Committee: Dr. M. Sam Mannan

Flammability limit is a significant safety issue for industrial processes. A certain amount of flammability limit data for pure hydrocarbons are available in the literature, but for industrial applications, there are conditions including different combinations of fuels at standard and non-standard conditions, in which the flammability limit data are scarce and sometimes unavailable.

This research is two-fold: (i) Performing experimental measurements to estimate the lower flammability limits and upper flammability limits of binary hydrocarbon mixtures, conducting experimental data numerical analysis to quantitatively characterize the flammability limits of these mixtures with parameters, such as component compositions, flammability properties of pure hydrocarbons, and thermo-kinetic values; (ii) Estimating flammability limits of binary hydrocarbon mixtures through CFT-V modeling prediction (calculated flame temperature at constant volume), which is based on a comprehensive consideration of energy conservation.

For the experimental part, thermal detection was used in this experiment. The experimental results indicate that the experimental results fit Le Chatelier's Law within experimental uncertainty at the lower flammability limit condition. At the upper flammability limit condition, Le Chatelier's Law roughly fits the saturated hydrocarbon mixture data, while with mixtures that contain one or more unsaturated components, a modification of Le Chatelier's is preferred to fit the experimental data. The easy and efficient way to modify Le Chatelier's Law is to power the molar percentage concentrations of hydrocarbon components.

For modeling prediction part, the CFT-V modeling is an extended modification of CAFT modeling at constant volume and is significantly related to the reaction vessel configuration. This modeling prediction is consistent with experimental observation and Le Chatelier's Law at the concentrations of lower flammability limits. When the quenching effect is negligible, this model can be simplified by ignoring heat loss from the reaction vessel to the external surroundings. Specifically, when the total mole changes in chemical reactions can be neglected and the quenching effect is small, CFT-V modeling can be simplified to CAFT modeling.

# ACKNOWLEDGEMENTS

I thank my committee members: Dr. M. Sam Mannan, my committee chair, for his guidance, advice, and encouragement; Dr. Kenneth R. Hall for his support and counsel; and Dr. Debjyoti Banerjee for his suggestions, availability and commitment.

I thank Dr. William J. Rogers for his friendly, insightful, detailed directions and comments of my experiment conductions.

A special thank you goes to my family for their love, support, encouragement, and patience, to people from Mary Kay O'Connor Process Safety Center for their help, support, and friendship.

# TABLE OF CONTENTS

Page

CHAPTER Page

# LIST OF FIGURES

FIGURE Page

FIGURE Page

FIGURE Page

# LIST OF TABLES

TABLE Page

# CHAPTER I

# INTRODUCTION

Flammable substances, which undergo exothermic reaction in the presence of air when exposed to an ignition source, are prevalent in today's chemical and petrochemical industries. Most hydrocarbons are extremely volatile under relatively normal operation conditions. To prevent workplace explosions of such flammable vapors, a detailed knowledge of the flammability is needed.

Accurate data on flammability limits and flash points are two significant issues for safety processes. Flammable substances are often provided with material safety data sheets. Flammability limits describe the composition of gas that can form propagating flames. Flash point describes the temperature at which a liquid develops flammable vapors. In industry, fire generally happens in the vapor or gas phase with a certain concentration in air. Compared with flash point, flammability limits attract more attention from our engineers.

The flammability limits data for pure hydrocarbons, which include lower flammability limits (LFL) and upper flammability limits (UFL), are adequate in the literature, but in industrial applications, there exist a variety of conditions including different temperatures, various pressures, varying oxygen contents, etc., in which the flammability limits data are scarce and sometimes unavailable. Furthermore, hydrocarbon mixtures with different components and different volume fraction are often

---

This thesis follows the style of Journal of Hazardous Materials.

encountered as well. So it is necessary and urgent to fill these gaps and build up comprehensive data sources for flammability limits.

Accurate flammability limit information is necessary for safe handling of flammable or combustible gas and liquid mixtures in industries. Theoretically, we can estimate flammability limits through experimental measurements, but experimental tests are usually time-and-money consuming, and sometimes impossible for the emergent requirements. Therefore, in order to estimate quantitative characteristics of flammability limits of hydrocarbon mixtures as a function of mixture composition and external conditions becomes necessary for safe operation. An empirical formula, Le Chatelier's Law, is the most widely used equation to calculate fuel mixtures' flammability limits based on the flammability limit data of pure components and molar fractions, while it exhibits application limits when fitted to non-standard conditions or when used to estimate upper flammability limits of some fuel combinations (from this research). Modifications of this equation and fits to the extended application conditions are profoundly valuable for industrial operations.

This research focuses on flammability limits (LFL and UFL) estimation for binary hydrocarbon mixtures in standard conditions basically (room temperature and ambient atmospheric pressure). Specifically, this research work is twofold: (i) Experiments to measure the LFLs and UFLs of binary hydrocarbon mixtures at standard conditions with different combinations of fuels (methane and ethylene, methane and n-butane, methane and acetylene, ethylene and propylene, ethylene and acetylene) and various molar fractions (0%-100%, 12.5%-87.5%, 25%-75%, 37.5%-62.5%, 50%-50%,

62.5%-37.5%, 75%-25%, 87.5%-12.5%, 100%-0%); Conduction of numerical data analysis from obtained experimental data, which includes modification of Le Chatelier's Law if necessary, or quantitatively relating the observed flammability limits to stoichiometric concentrations of fuel mixtures, or connecting combustion heat with the measured flammability limits, external conditions, chemical properties and molar fraction ratios of hydrocarbon mixtures, (ii) Modeling to predict flammability limits of binary hydrocarbon mixtures using thermo-kinetic theories and through energy conservation applications. Specifically, a comprehensive energy balance was applied at constant volume reactor based on its configuration. This modeling can be simplified to Calculated Adiabatic Flame Temperature (CAFT) modeling if the heat loss from the reactor is negligible and total molar amounts keep constant in the reactor.

The following chapters consist of: Chapter II, background which gives some basic information about flammability limits, e.g., definition, properties, existing methods to measure flammability limits and existing models to predict the flammability limits; Chapter III, experimental apparatus and procedures, which describe the experimental setup and configuration, experimental method and estimation criterion to determine the flammability limits of binary hydrocarbon mixtures; Chapter IV, experimental results including LFLs and UFLs of binary hydrocarbon mixtures at standard conditions, and numerical data analysis based on the experimental observations that include modification of Le Chatelier's Law at the concentrations of upper flammability limits, quantitative relation of LFLs and UFLs to the stoichiometric concentrations; Chapter V, calculated flame temperature at constant volume modeling construction (CFT-V), use of

CFT-V modeling to predict the LFLs of binary hydrocarbon mixtures, and comparison of the results from experimental observations and modeling predictions ; Chapter VI, conclusions from experimental results and modeling predictions, and future studies based on current information from this research.

# CHAPTER II

# BACKGROUND

## 2.1 Definition of Flammability Limits

Flammability limits, sometimes referred to as explosion limits [1], are defined as the concentration range in which a flammable substance can produce a fire or explosion when an ignition source (such as a spark or open flame) is present. The concentration in air is generally expressed as percentage fuel by volume in the vapor phase. Additionally, flammability limits are divided into two types: (i) the upper flammable limit (UFL) above which the fuel concentration is too rich (deficient in oxygen) to burn; (ii) the lower flammability limit (LFL) below which the fuel concentration becomes too lean (sufficient in oxygen) to be ignited. Usually, the limits are experimentally obtained by determining the limiting mixture compositions between flammable and non-flammable mixtures [2], that is,

$$LFL_{T,P} = \frac{1}{2}(C_{g,n} + C_{l,f}) \tag{1}$$

$$UFL_{T,P} = \frac{1}{2}(C_{g,f} + C_{l,n}) \tag{2}$$

where $LFL_{T,P}$, $UFL_{T,P}$ are lower flammability limit and upper flammability limits at specific temperature and pressure; $C_{g,n}$, $C_{l,n}$ are greatest concentration and least concentration of fuel in oxidant that are nonflammable; $C_{l,f}$, $C_{g,f}$ are greatest concentration and least concentration of fuel in oxidant that are flammable.

## 2.2 Dependences of Flammability Limits

As with most aspects of flammability, the evaluation of flammability limits is not absolute, but rather depends on the details of test apparatus and experiment conditions by which the determination is made. There are no definite parameters to quantitatively characterize the flammability limits. In practice, the limits of flammability of a particular system of air-fuel are affected by a variety of factors including temperature, pressure, oxygen concentration, inert gas concentration, size of equipment, direction of flame propagation, turbulence, gravitational field strength, etc [3].

### 2.2.1 Flammability Limits and Temperature

Research on combustible gases and vapors by Zabetakis [4] indicated that the flammability limits of most fuels are not stable at different external temperature. Specifically, when external temperature goes up, the lower flammability limits will decrease while the upper flammability limits increase. In industrial operations, occasionally some fuel-air mixtures become flammable although they stay outside of flammability limits. The possible reason is temperature change, which trigger the variation of fuel-air mixtures from nonflammable at initial temperature to flammable at elevated temperature heated by an ignition source. Figure 2.1 shows this variation from Point A to Point B.

In 1951, Zabetakis et al. observed that for most hydrocarbons the LFL decreases by about 8% for each 100 ºC rise in mixture temperature [5]. By this rule, mixtures containing an infinitesimal concentration of fuel could sustain flame propagation if the temperature was raised to about 1275 ºC (25 + 100/0.08), which was confirmed by the

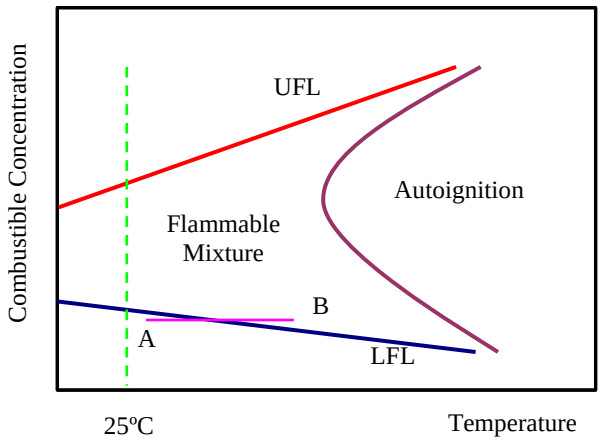


Fig. 2.1. Effects of temperature on flammability limits. (Source: Zabetakis, M.G., 1965 [4])

future work at the Bureau of Mines (BM) [4]. Using this value, if the LFL is known at room temperature $T_1$ (25 ºC), then it can be evaluated at another temperature $T_2$ according to Eq. (3). For the UFL, BM recommends that the increase with temperature be computed by Eq. (4) [4]. However, while the predicted temperature effect on the LFL is very similar to the measured data, for UFL there are substantial discrepancies. Even the higher alkanes (hexane, heptane, and octane) do not follow the general relationship. One reason that nonlinearities arise is due to cool-flame ignitions with some gases, at some temperatures, and not at others [6].

$$\frac{LFL_{T_2}}{LFL_{25}} = 1 - 0.000784(T_2 - 25) \tag{3}$$

$$\frac{UFL_{T_2}}{UFL_{25}} = 1 + 0.000721(T_2 - 25) \tag{4}$$

The data may also be fairly well correlated by the modified Burgess-Wheeler law, suggested by Zabetakis, Lambiris and Scott for the effect of temperature on the LFL and

UFL of hydrocarbons in the absence of cool flames, which is expressed by Eq. (5) and Eq. (6) [7], where $\Delta H_C$ is the net heat of combustion (kcal/mole) and T in ºC.

$$LFL_T = LFL_{25} - \frac{0.75}{\Delta H_C}(T - 25) \quad (5)$$

$$UFL_T = UFL_{25} + \frac{0.75}{\Delta H_C}(T - 25) \quad (6)$$

2.2.2 Flammability Limits and Pressure

Generally, pressure has only a slight effect on LFL except at low pressure (<50 mmHg absolute), where flames do not propagate, while the UFL increases considerably as the initial pressure increases [8]. Raising the initial pressures of the fuel-gas system can generally broaden its flammability limit range, put differently, lowering LFL and raising UFL. The relations can be represented by formulas as follows (E.q (7) and E.q. (8)) [9]. Melhem computed flame temperatures for several gases as functions of concentration and pressure, and observed that increasing pressures raises the flame temperature for fuel-rich mixtures, but not for lean ones [10]. Thus, if the flame temperature is assumed to be constant at the flammability limits, then the UFL will rise with increasing pressure, but the LFL will not change. Figure 2.2 shows the initial pressure effects on the flammability limits of natural gas [4]: the LFL reduces slightly at a highly extended pressure while UFL experiences a significant change, which is consistent with the basic principle of pressure effect on flammability limits.

$$LFL_P = LFL_{1atm} - 0.31 \ln P \quad (7)$$

$$UFL_P = UFL_{1atm} + 8.9 \ln P \quad (8)$$

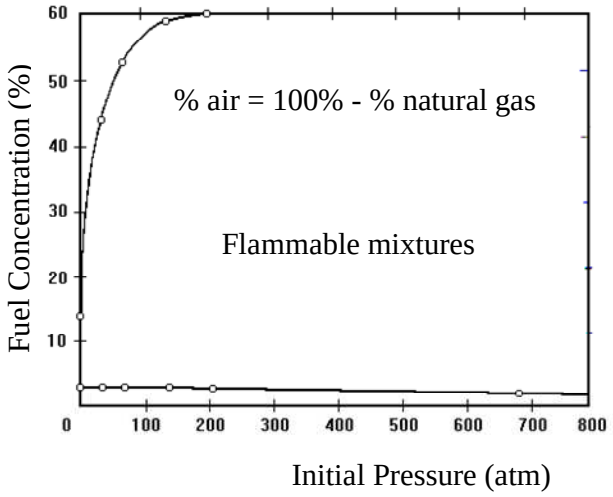


Fig. 2.2. Effect of initial pressure on flammability limits of natural gas at 28 ºC. (Source: Zabetakis, M.G., 1965 [4])

2.2.3 Flammability Limits and Oxygen Concentration

In industrial operation with flammable or combustible fuels, controlling oxygen content at a certain level that prevents the ignition of flammable vapor is a critical criterion to chemical safety processes, because flammability limits vary with oxygen concentration. Normally, the LFLs in a variety of oxygen concentrations are almost same as in air. Since the LFL is a fuel-lean condition, excess oxygen is available at 21% and any further excess oxygen is simply acting as a diluent. The molar heat capacities of oxygen and nitrogen are similar, and consequently the LFL value is not changed by going to a 100% oxygen atmosphere. However, the UFLs increase sharply with increasing oxygen concentrations. As we dilute oxygen concentration in air continuously, the LFL and UFL converge at one point, where oxygen concentration is called minimum oxygen concentration (MOC) below which the fuel-air mixtures can not support sustained combustion no matter how large the ignition energy is input. Figure

2.3 indicates the relationship between flammability limits and varied oxygen concentration in methane-oxygen-nitrogen system [4].

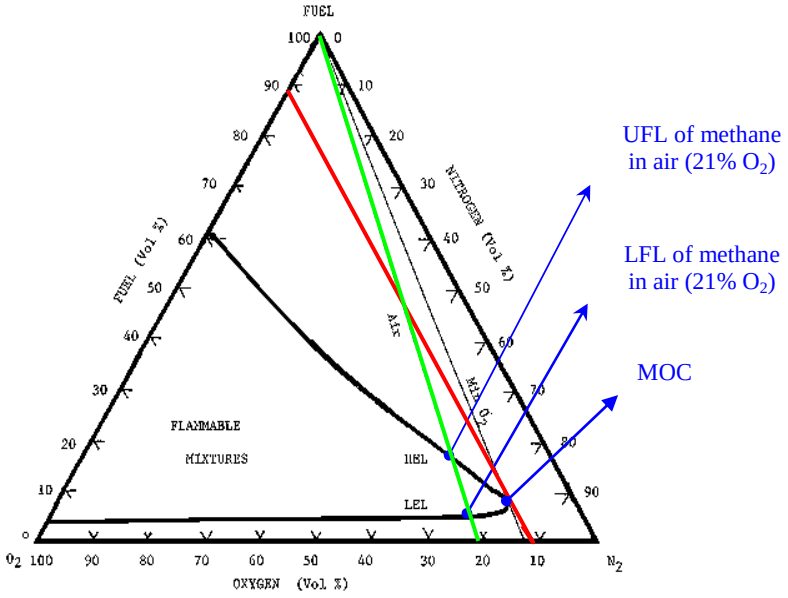


Fig. 2.3. Flammability limits diagram with varying $O_2$ concentrations. (Source: Zabetakis, M.G., 1965 [4])

2.2.4 Flammability Limits and Inert Gases

Any flammable material present in air must be present at a concentration higher than the LFL and lower than the UFL for a fire or explosion occurrence. To control the fire and explosion, inert additives (that is, substances which are neither fuels nor oxidizers) are sometimes added to mixtures in order to decrease their flammability limits or make the mixture entirely outside the range of flammability. Besnard's report provides an excellent example for the influence of inert gases on the flammability limits [11]. He systematically investigated a number of inert gases which have different inactivating capacities to reduce the flammable range of flammable fuel-air mixtures.

One of the experimental results is summarized in Figure 2.4, which shows the variations of flammability limits of methane in air at standard conditions with the addition of a group of inert gases. From this figure it can be seen that, for moderate amounts of inert additives, the effect is mainly on the UFL except chemical $C_2H_2F_4$. All of the additives are able to make a mixture non-flammable if added in sufficient quantities. For most hydrocarbon gases, nitrogen in the amount of 40-50 vol % must be added to a fuel/air mixture in order to make them nonflammable, that is, to prevent flame propagation [4]. These are very high amounts, whereas much lower concentrations are sufficient when using many halogen-containing gases.

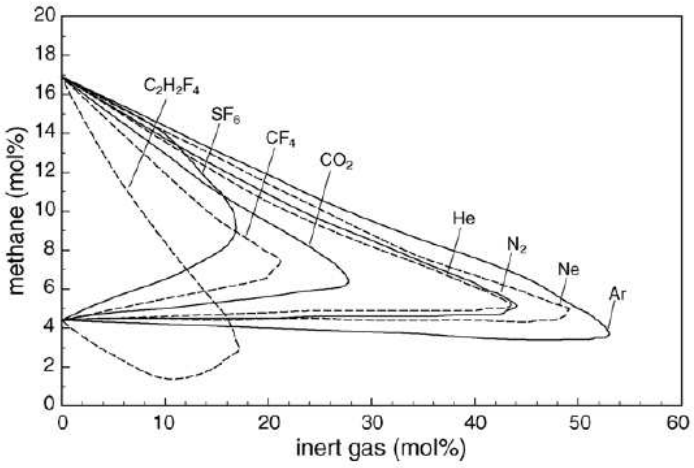


Fig. 2.4. Influence of inert gases on the flammability limits of methane in air at standard conditions. (Source: Besnard, S., 1996 [11])

2.2.5 Flammability Limits and Experimental Apparatus Sizing

For a period time of two hundred years, experiments have been conducted to measure the flammability limits by using different apparatus. The results show that flammability limits are relatively dependent on the experimental apparatus sizes [12].

Coward and Jones [13] used a cylindrical vertical tube of 5 cm diameter to measure the flammability limits for a wide variety of gases and vapors. Later, Zabetakis [4] suggested that a tube diameter of 5 cm is too small for measuring the flammability of halogenated hydrocarbons. A comprehensive research on flammability limits changing with vessel size and shape was performed, and basic results were summarized as [14]: (i) For a cylindrical vessel of small diameter with a large height, the flammability limits are primarily determined by the quenching effect of the wall; (ii) For cylindrical vessels of

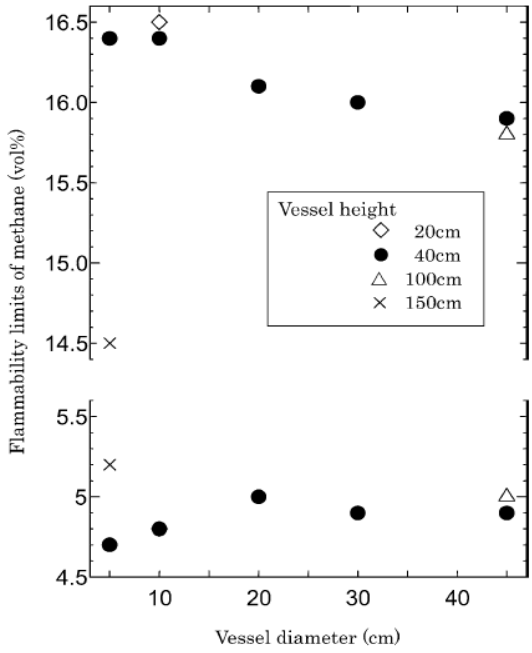


Fig. 2.5. Flammability limits of methane in various vessels with different sizes and shapes. (Source: Takahashi, A., et al., 2003 [14])

small heights, the flammability limits are affected by hot gas accumulation at the vessel ceiling, unburnt gas heating, self heating of the incipient flame, and the quenching effect of the walls; (iii) if the vessel size is large enough, all of these effects become negligible, the experimental values of flammability limits may approach the values that would be

obtained in free space. Figure 2.5 shows the relationship methane's flammability limits vary with vessel size [14].

2.2.6 Flammability Limits and Ignition Energy

Flammable gas/vapor mixtures need initial ignition energy to combust. The minimum energy required to start burning of flammable gas mixture is called Minimum Ignition Energy (MIE). In general, many flammable mixtures can be ignited by sparks having a relatively small energy content (1 to 100 mJ) but a large power density (greater than 1 megawatt / $cm^3$) [4]. Figure 2.6 illustrates the effect of mixture composition on the spark energy requirements for ignition of methane-air mixture [15]. The mixture compositions that depend on the ignition source strength are defined as ignition limits,

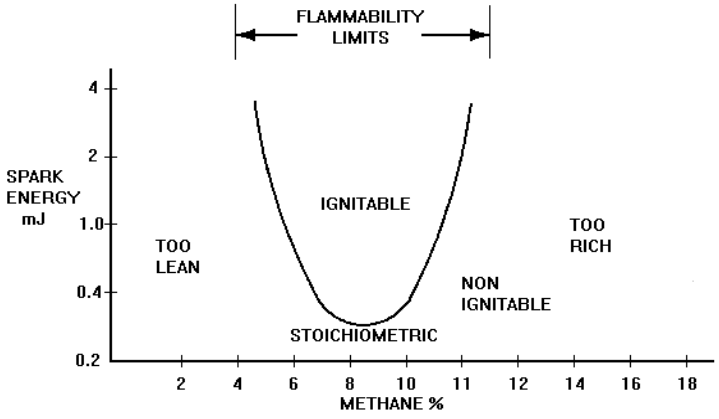


Fig. 2.6. Ignition curve and flammability limits for methane-air mixtures at atmospheric pressure and 26 °C. (Source: Guest, P.G., et al., 1952 [15])

which are indicative of the ignition ability of the energy source. Different from ignition limits, the flammability limits are essentially independent of the ignition source strength,

therefore considerably greater spark energies are required to establish flammability limits than those required for limits of ignitibility [16].

2.2.7 Flammability Limits and Propagation Direction

By 1902, both Clowes [17] and Eitner [18] had demonstrated that limits are wider for upward than for downward flame propagation. In 1914 Leprince-Ringuet showed that the horizontal limit lies between the upward and downward limits [12]. Close to the flammability limits, flame cannot travel downward, because buoyancy creates an upward convective current. But upward propagation can remain possible, since buoyancy aids propagation. For fundamental combustion chemistry studies, downward propagation is preferred precisely because the extra effects of buoyancy do not come into play, but for industrial interest, upward flame propagation is

Table 2.1. Effect of propagation direction on flammability limits. (Source: White, A.G., 1924 [19])

| **Mixture** | **Direction** | **LFL** (vol%) | **UFL** (vol%) |
|---|---|---|---|
| methane/air | Upward | 5.35 | 14.85 |
| | Horizontal | 5.40 | 13.95 |
| | Downward | 5.95 | 13.35 |
| pentane/air | Upward | 1.42 | 8.0 |
| | Horizontal | 1.44 | 7.45 |
| | Downward | 1.48 | 4.64 |
| benzene/air | Upward | 1.45 | 7.45 |
| | Horizontal | 1.46 | 6.65 |
| | Downward | 1.48 | 5.55 |

recommended [9]. The data of Table 2.1 show that the UFL values are much more affected by the direction than the LFL values, in which the differences are mostly within experimental data scatter [19].

#### 2.2.8 Flammability Limits and Turbulence

From previous research, there exists a limited amount of data suggesting that turbulence can narrow the flammability range for pure fuel gases/vapors. When fan-stirring was introduced into a test chamber, it was found that the LFL rose while UFL fell with fan speed and consequently with the turbulence velocity [20, 21]. The effect requires a sizable stirring speed, however, to become significant. The narrowing effect on observed flammability limits has been interpreted as being an MIE impact: if the experiments are conducted at the same ignition energy and it requires more energy to ignite mixtures that are either turbulent or have an equivalent ratio far away from stoichiometric concentration, then turbulent mixtures will be observed as having a smaller flammability range [20].

## 2.3 Flammability Limits Measurement

### 2.3.1 Methods to Measure Flammability Limits

Previously, the flammability limits were determined by visual identification. This criterion for flammability limits estimation is flame propagation from the point of ignition to a certain distance. The best known experimental method using visual identification for measuring flammability limits of premixed gases is that developed by BM [13]. It contains of a 50 mm I.D. glass tube, 1.5 m long. For a mixture to be declared flammable, propagation has to occur at least half way up the tube; if only a shorter

propagation distance is observed, this is deemed to occur due to localized heating from the igniter, and is not considered representative of the substance. By using this method, the U.S. Bureau of Mines generated a large body of flammability limits data for pure gas as well as some gas mixtures. Much of the work was done and summarized by Coward and Jones [13], Zabetakis et al. [4], and Kuchta et al. [6] through Bureau of Mines Bulletin publications.

In recent years, apparatus with closed, steel, spherical reaction vessels and center ignition also have been used for flammability limit determinations. Unlike visual detection criterion, in this method the detection criterion is the relative pressure increase in reaction vessel resulting from combustion. Burgess et al. in 1982 published data from a 25,500 L sphere vessel that incorporated a 7% pressure rise criterion [22], and Cashdollar et al. in 2000 published data from 20 L and 120 L chambers with 3% and 7% pressure rise criteria [23].

Flammability limits also have been tested indirectly using counterflow burners, where twin gas jets of premixed fuel and oxidizer are released from opposing nozzles against each other, and ignited to produce twin, planar flames. The average gas exit velocity, often called stretch rate, is measured at different fuel concentrations. The fuel concentration is plotted as a function of stretch rate. The fuel concentration is extrapolated linearly to a stretch rate of zero, and the intercept is taken as the flammability limit [24].

2.3.2 Standardization of Flammability Limits Measurement

The methods of measuring the flammability limits of gases have been known well for a long time, and there have been many attempts to standardize the measurement methods to improve compatibility of flammability data. However, no standard method for that measurement has been estimated yet.

In U.S., the American Society for Testing and Materials (ASTM) adopted three closed vessel methods to measure flammability limits of gases and vapors: (i) ASTM E 681, using a 5 L glass sphere to determine the flammability limits of substances in air at 1 atm or lower pressure and at temperature below 150 ºC with a high voltage, central spark as the ignition source; the flame is required to show self-propagation independent of the plume of hot gas created by the ignition source [25]. (ii) ASTM E 2079, requiring a 4 L or larger near-spherical vessel placed in a heating oven with a 10 J or greater ignition source, and 7% total pressure rise criterion at varying oxygen content. The purpose of the test is solely to establish MOC, so various concentrations of oxygen are supplied by trial-and-error until the minimum value is found [26]. (iii) ASTM E 918, requiring a 1 L and 76 mm diameter minimum vessel inside an insulated oven with a fuse wire igniter near the bottom, and a 7% total pressure rise criterion at elevated temperature (up to 200 ºC) and pressure (1.38 Mpa) [27].

In European, the current standard methods for flammability limit determination are DIN 51649 and EN 1839 (subdivided into EN 1839 T and EN 1839 B). The DIN 51649 test method uses a 6 cm diameter, 30 cm tall glass cylinder opened at the top with a spark igniter (0.5 s, 10 W) at the bottom. The criterion for flammability is any visual

sign of flame detachment from the ignition source. The EN 1839 T method uses an 8 cm wide, 30 cm tall, open top glass cylinder, with spark igniter at the bottom (0.2 s and 10 W). The criterion for flammability is propagation of flame 10 cm vertically above the igniter or 12 cm in the horizontal direction at any point of the flame path. EN 1839 B allows the use of a cylinder or spherical vessel of at least 5 L and an exploding fuse wire (0.2 s, 10-20 J) in the center. The criterion for flammability is a 5% minimum pressure rise after ignition [28].

## 2.4 Modeling to Estimate Flammability Limits

Flammability limits are the most important safety specifications that must be considered in assessing the overall flammability hazard potential of chemical substances in storage, processing, and handling. Ideally, experimental data for flammability limits of substances are always needed; however, they are scarce or sometimes unavailable, especially in a variety of industrial operation conditions. To satisfy the requirements from various industrial process operations, some formulas and predicting models were developed by summarizing experimental results or theoretical derivation, which include Shimy's Equations, Calculated Adiabatic Flame Temperature (CAFT) Modeling, F-Number Modeling, Structural Group Contribution (SGC) Modeling, and Le Chatelier's Law and its Modification.

### 2.4.1 Shimy's Equations.

Based on former researchers' work, Shimy [29] pointed out that flammability limits are function of constituting atoms for fuels. He gave some empirical equations to estimate the lower flammability limit and upper flammability limit separately for various

chemicals at atmospheric pressure and room temperature. The results are noted in table 2.2. In Shimy's equations, the lower flammability limit is only dependent on the numbers of carbon atoms, while the upper flammability limit is associated with the numbers of carbon atoms, hydrogen atoms in radicals, and hydrogen atoms not in radicals.

Table 2.2. Shimy's Equations for flammability limits estimation at standard conditions. (Source: Shimy, A.A., 1970 [29])

| | **LFL** | **UFL** |
|---|---|---|
| Paraffinic Hydrocarbons and Olefins | $\frac{6}{nC^{a}} + 0.2$ | $\frac{60}{nH^{b}} + \frac{nC}{20} + 2.2$ |
| Iso-Hydrocarbons | $\frac{6}{nC} + 0.1$ | $\frac{60}{nH} + 2.3$ |
| Benzene Series | $\frac{8}{nC}$ | $\frac{86}{2nH_{r}^{c} + nH'^{d}}$ |
| Alcohols | $\frac{6}{nC} - 0.7$ | $\frac{80 - 2nH}{2nC} + 3$ |

[a] *nC* is the number of carbon atoms
[b] *nH* is the number of hydrogen atoms
[c] *nHr* is the number of hydrogen atoms in radicals
[d] *nH′* is the number of hydrogen atoms not in radicals

### 2.4.2 CAFT Modeling

Calculated adiabatic flame temperature is the temperature that is obtained, when there are no combustion heat losses, or the enthalpy remains constant. Edgerton and Powling [30] observed that lower paraffins have a nearly constant flame temperature, and later Stull [31], Hansel [32] and Melhem [33] used this approach to predict flammability limits. Now CAFT has become a powerful tool to estimate the lower

flammability limit of gas mixtures. To estimate the flammability limits, a temperature threshold is assumed. Some researchers agree that this temperature is around 1550 K [34] or 1200 K [35], while others believed that this temperature is in the range of 1000-1500 K [10]. Due to the similarity of critical reaction temperatures among organic substances, Mashuga and Crowl [36] found that a temperature of 1200 is a good criterion for the prediction of the flammability zones for methane and ethylene; Shebeko et al [34] selected the temperature 1600 K in obtaining formulas for lower flammability limit calculations. By using Vidal et al.'s provided methodology [37], we can mathematically derive the lower flammability limit as follows. The methodology was previously presented by Shebeko at al [34], where an overall adiabatic temperature of 1600 K was used for the estimation of the lower flammability limits.

$$LFL = \frac{100}{1 + v_{ao}} \tag{9}$$

where $v_{a0}$ is the number of moles of air per mole of fuel in the mixture at the lower flammability limit.

The flammability limit is associated with a certain critical reaction temperature, which can be assumed to be equivalent to the adiabatic flame temperature, $T_{ad}$ at the lower flammability limit composition and is the maximum temperature achieved due to the combustion reaction when the fuel composition is equal to lower flammability limit. By using energy balance equation, we have,

$$\sum_i H_{reac,i}(T_i, P) = \sum_i H_{prod,i}(T_{ad}, p) \tag{10}$$

where $H_{reac,i}$ and $H_{prod,i}$ are the enthalpies of the reactant *i* and product *j*; $T_i$ is the initial temperature, $T_{ad}$ is the adiabatic flame temperature which is equal to final temperature. Expanding Eq. (10) by a given fuel $C_nH_mO_l$ reacting with air, we can get,

$$H_f^i + v_{a0}H_a^i = nH_{CO_2}^{ad} + \frac{m}{2}H_{H_2O}^{ad} - \beta H_{O_2}^{ad} + v_{a0}H_a^{ad} \tag{11}$$

where $H_f, H_a, H_{CO_2}, H_{H_2O}$ and $H_{O_2}$ are the absolute mole enthalpies of fuel, air, carbon dioxide, steam, and oxygen; $\beta$ is the stoichiometric coefficient of oxygen in the reaction of complete combustion; superscripts *i* and *ad* refer to the initial and final conditions, respectively. Solving $v_{a0}$ from Eq. (11) and putting it into Eq. (9), we can get the calculate lower flammability limits as follows,

$$LFL = \frac{100}{1 + g_f\Delta H_f + g_C n + g_H m + g_O l} \tag{12}$$

where,

$$\left.\begin{array}{ll} g_f = \dfrac{1}{H_a^{ad} - H_a^i} & g_C = g_f(H_C^i - H_{CO_2}^{ad} + H_{O_2}^{ad}) \\ g_H = 0.5g_f(H_{H_2}^i - H_{H_2O}^{ad} + 0.5H_{O_2}^{ad}) & g_O = -0.5g_f(H_{O_2}^{ad} - H_{O_2}^i) \end{array}\right\} \tag{13}$$

2.4.3 SGC Modeling

The theoretical concept of the SGC approach has been explained by Benson and Buss [38]. Reid et al. [39] have mentioned that this approach is a powerful tool for predicting properties of pure substances and multi-component mixtures. The examples include critical temperature, critical pressure, critical volume, boiling point, freezing point, viscosity, thermal conductivity, and Gibbs free energy. Albahril [40] pointed out

that the flammability properties are some of the macroscopic properties of compounds that are related to the molecular structure. The relevant characteristics of molecular structure are related to the atoms, atomic group, and bond types. To them, we can assign weighting factors and then determine the property, usually by an algebraic operation which sums the contributions from the molecule's parts. Albahril gave the following equation to quantitatively characterize the flammability limits [40].

$$\Phi = a + b\left(\sum_i \Phi_i\right) + c\left(\sum_i \Phi_i\right)^2 + d\left(\sum_i \Phi_i\right)^3 + e\left(\sum_i \Phi_i\right)^4 \quad (14)$$

where $\Phi$ refers to lower flammability limit or upper flammability limit, $\Phi_i$ is the molecular structure group contributions (Table 2.3) for lower flammability limit or upper flammability limit, *a, b, c, d,* and *e,* are constants, which are presented in Table 2.4.

Table 2.3. Group contribution for estimation of upper and lower flammability limits. (Source: Albahri, T.A., 2003 [40])

| HC type | Serial no. | Group | $(UFL)_i$ | $(LFL)_i$ |
|---|---|---|---|---|
| Paraffins | 1 | –$CH_3$ | −0.8394 | −1.4407 |
| | 2 | >$CH_2$ | −1.1219 | −0.8736 |
| | 3 | >CH– | −1.2598 | −0.2925 |
| | 4 | >C< | −2.1941 | 0.2747 |
| Olefins | 5 | =$CH_2$ | 0.2479 | −1.3126 |
| | 6 | =CH– | −0.3016 | −0.7679 |
| | 7 | >C= | −0.6524 | −0.2016 |
| | 8 | =C= | 0.0675 | −0.4473 |
| | 9 | ≡CH | 3.8518 | −1.2849 |
| | 10 | ≡C– | 1.3924 | −0.4396 |
| Cyclic | 11 | >$CH_2$ | −0.8386 | −1.0035 |
| | 12 | >CH– | −0.9648 | −0.4955 |
| | 13 | >C > | −2.2754 | 0.1058 |
| | 14 | =CH– | −0.0821 | −0.8700 |
| | 15 | >C= | −0.1252 | −0.5283 |
| Aromatics | 16 | =CH– | −1.2966 | −0.8891 |
| | 17 | >$CH_2$ | −1.6166 | −1.0884 |
| | 18 | >C= (fused) | −1.4722 | −0.3694 |
| | 19 | >C= (nonfused) | 0.6649 | −0.2847 |

.

Table 2.4. Coefficients for Eq. (16). (Source: Albahri, T.A., 2003 [40])

| Property | Use with table | *a* | *b* | *c* | *d* | *e* |
|---|---|---|---|---|---|---|
| FPT | 3 | 84.65 | 64.18 | −5.6345 | 0.360 | −0.0101 |
| AIT | 4 | 780.42 | 26.78 | −2.5887 | −0.3195 | −0.007825 |
| UFL | 5 | 18.14 | 3.4135 | 0.3587 | 0.01747 | 3.403E-04 |
| LFL | 5 | 4.174 | 0.8093 | 0.0689 | 0.00265 | 3.76E-05 |

2.4.4 F-Number Modeling

F-Number model is a novel method of predicting flammability limits proposed by Kondo et al [41]. The F-Number is an index to address the flammability characteristics in terms of one unique number for each substance. The definition of F-number is as follows:

$$F = 1 - \left(\frac{L}{U}\right)^{0.5} \tag{15}$$

where $L$ is the lower flammability and $U$ the upper flammability limit. From Eq. (15), we can see F-Number takes values ranging from zero to unity depending on the degree of flammability of substances. Therefore, the F-Number can be utilized to classify the hazardous properties of flammable gases and vapor. Basically, flammable gases with F-Number value of 0.0-0.2 are treated as vaguely flammable, those of 0.2-0.4 weakly flammable, those of 0.4-0.6 normally flammable, those of 0.6-0.8 strongly flammable, and those of 0.8-1.0 super flammable [41].

According Kondo's suggestion [41], the F-Number can be obtained using Eq. (16). The lower flammability limit and upper flammability limit can be calculated by Eq. (17), and Eq. (18).

$$F = p_1 \times \begin{pmatrix} 1 + p_2 C_1 + p_3 R_{OE} + p_4 R_{CO} \\ + p_5 R_{COO} + p_6 R_{NH} + p_7 R_{RNG} \\ + p_8 R_{ARM} + p_9 R_{US} \end{pmatrix} \times \begin{pmatrix} 1 + p_{10} R_F + p_{11} R_{Cl} + p_{12} R_{Br} \\ + p_{13} R_{OH} + p_{14} R_{NO_2} + p_{15} R_{NH_2} \\ + p_{16} R_{CN} + p_{17} R_{COOH} \end{pmatrix} \quad (16)$$

where, $C_1$ takes the value of one or zero according to whether the molecule is a compound of mono-carbon skeleton or not; however, the methane derivatives that contain *CO*, *COO*, *CN*, or *COOH* group are treated exceptionally, and $C_1$ will take the value of zero for these compounds; $R_{OE}$, $R_{CO}$, $R_{COO}$, and $R_{NH}$ denote numbers of ether, carbonyl, ester, and imine group, respectively, divided by the total number of skeletal carbons; $R_{RNG}$ and $R_{ARM}$ denote numbers of aliphatic and aromatic rings divided by the total number of skeletal carbons. $R_{US}$ denotes the total number of unsaturations in the carbon skeleton including aliphatic and aromatic rings divided by the total number of skeletal carbons; $R_F$, $F_{Cl}$, …, and $R_{COOH}$ denote number of *F*, *Cl*, …, and *COOH* divided by the total number of hydrogen atoms in the corresponding pure hydrocarbon molecule. $p_1$-$p_{17}$ are constants shown in Table 2.5.

Table 2.5 Coefficients for Eq. (18). (Source: Kondo, S., et al., 2001 [41])

| No. | Description | Obtained value | S.E. |
|---|---|---|---|
| $p_1$ | Main coefficient | 0.581 | 0.009 |
| $p_2$ | If one carbon | −0.194 | 0.046 |
| $p_3$ | Ether | 0.134 | 0.089 |
| $p_4$ | Carbonyl | 0.028 | 0.091 |
| $p_5$ | Ester | −0.097 | 0.071 |
| $p_6$ | NH | −0.014 | 0.151 |
| $p_7$ | Aliphatic ring | 0.299 | 0.152 |
| $p_8$ | Aromatic ring | −0.125 | 0.296 |
| $p_9$ | Unsaturation | 0.290 | 0.069 |
| $p_{10}$ | F | −0.344 | 0.114 |
| $p_{11}$ | Cl | −0.985 | 0.098 |
| $p_{12}$ | Br | −3.160 | 0.482 |
| $p_{13}$ | OH | 0.284 | 0.256 |
| $p_{14}$ | $NO_2$ | 0.527 | 0.373 |
| $p_{15}$ | $NH_2$ | −0.344 | 0.263 |
| $p_{16}$ | CN | −0.566 | 0.349 |
| $p_{17}$ | COOH | −0.850 | 0.351 |

$$LFL = (UL)^{0.5}(1-F) \tag{17}$$

$$UFL = \frac{(UL)^{0.5}}{1-F} \tag{18}$$

where $(UL)^{0.5}$ is a function of the chemical formula of a general molecule given by $C_iH_jO_kF_lCl_mBr_nN_p$, which is close to the stoichiometric concentration $C_{st}$. But some data analysis indicated that the $C_{st}$ is not always a good approximation to the value of $(UL)^{0.5}$. Eq. (19) gives the correction for $C_{st}$ and $(UL)^{0.5}$.

$$\frac{(UL)^{0.5} - C_{st}}{C_{st}} = 0.00472(M - 32.00) \tag{19}$$

where $M$ is the molecular weight. If $C_iH_jO_kF_lCl_mBr_nN_p$ completely reacts with the products $CO_2$, $H_2O$, $HF$, $HCl$, $Br_2$ and $N_2$, $C_{st}$ can be expresses as Eq. (20); and if the products $CO_2$, $H_2O$, $HF$, $Cl_2$, $Br_2$ and $N_2$, $C_{st}$ is Eq. (21).

$$C_{st} = \frac{1}{1 + 4.773\left[i + \left(j - l - m - 2k\right)/4\right]} \tag{20}$$

$$C_{st} = \frac{1}{1 + 4.773\left[i + \left(j - l - 2k\right)/4\right]} \tag{21}$$

2.4.5 Le Chatelier's Law and Its Modification

Le Chatelier arrived at his mixture rule for lower flammability limit of gas mixture from his experiments with methane and other lower hydrocarbons [42]. The proposed empirical mixing rule is expresses as Eq. (22)

$$LFL_{mix} = \frac{1}{\sum_{i=1}^{N} \frac{y_i}{LFL_i}} \tag{22}$$

where $y_i$ is the mole fraction of the $i^{th}$ component considering only the combustible species, and $LFL_i$ is the lower flammability limit of the $i^{th}$ component in volume percent, $LFL_{mix}$ is the lower flammability limit of the gas mixtures. Algebraically, Le Chetelier's method states that the mixture flammability limit has a value between the maximum and minimum of the pure component flammability limits.

In addition, Kondo et al. [43] have shown that Le Chatelier's Law can be extended to upper flammability limit estimation for some blended fuels with acceptable accuracy. That is,

$$UFL_{mix} = \frac{1}{\sum_{i=1}^{N} \frac{y_i}{UFL_i}} \tag{23}$$

However, since Le Chatelier's method is intrinsic for blended gases containing only flammable compounds, it is not applicable as mixing flammables containing inert gases. Kondo et al. [43] also developed an extended Le Chatelier's formula to explain the inert gas dilution effect on the flammability limits of flammable gases. Eq. (24) and Eq. (25) are specifically applicable to blend gases consisting of one flammable gas and one diluent gas.

$$\frac{C_1}{LFL_{fuel}} = \frac{C_1}{LFL_1} + pC_{in} \tag{24}$$

$$\frac{C_1 n_1}{100 - (UFL_{fuel} / C_1)} = \frac{C_1 n_1}{100 - UFL_1} + qC_{in} + rC_{in}^2 + sC_{in}^3 \tag{25}$$

where $LFL_1$ and $UFL_1$ are lower flammability limit and upper flammability limit of fuel in air; $LFL_{fuel}$ and $UFL_{fuel}$ are lower flammability limit and upper flammability limit of

fuel-inert gas mixtures; $C_1$ and $C_{in}$ are the mole fraction of the fuel gas and inert gas in the fuel-inert blend ($C_{in} = 1 - C_1$); *p*, *q*, *r*, *s* are parameters to be determined experimentally.

# CHAPTER III

# FLAMMABILITY APPARATUS AND EXPERIMENTAL PROCEDURES

## 3.1 Introduction

Nearly 200 years' research has been carried out to develop the existing flammability limit measurements, in which the popularly used detection criteria of visual identification, and relative pressure rise were applied. Even though there were different experimental configurations, measurement methods, and detection criteria, the most widely accepted definition of flammability limits, or self-sustained flame propagation in fuel-oxidant mixtures, is treated as the key point for experimental measurement of fuel-lean condition (LFL) and fuel-rich condition (UFL), at which flame can propagate to a certain distance.

Knowledge of flammability limits is important and necessary for evaluation of potential fire and explosion hazards. In the accumulated literature, many investigations have been performed on the flammability limits for pure fuels; however, there are only some scattered flammability data of fuel mixtures, and generally these data are scarce. Untill now, Le Chatelier's has been the simplest and most useful formula for fuel mixture flammability limit estimation. Mashuga and Crowl [44] gave the theoretical derivation of Le Chatelier's mixture rule for flammability limits with many assumptions, which can roughly fit the experimental conditions at the lower flammability limits. When applying these similar assumptions to the upper flammability limit conditions, poor to moderate results could be obtained depending on the fuel species.

Wong [46] constructed the experimental apparatus for flammability limits measurement, and evaluated the effectiveness of this experimental setup by measuring the flammability limits of some pure hydrocarbon gases (methane, butane, ethylene and propylene). This research focuses on the flammability limit data collection from binary hydrocarbon mixtures by applying Wong's experimental setup, and then conducting numerical analysis of experimental data.

This research measured the flammability limits of fuel mixtures using fuel combinations of some typical saturated hydrocarbon gases (methane, n-butane), unsaturated hydrocarbon gases with double carbon-carbon bonds (ethylene, propylene) and triple carbon-carbon bonds (acetylene). The observation results were fit to Le Chatelier's law, and a modification of Le Chatelier's law was used when the experimental results exhibit large deviations from Le Chatelier's predictions.

**3.2 Flammability Apparatus**

The flammability apparatus used in this research is a device used to measure flammability limits of fuel and fuel mixtures. It was developed by Wong [46] at Texas A&M University. A schematic configuration of the flammability apparatus is showed in Figure 3.1. The key design feature consists of five parts: (i) Reaction vessel; (ii) Gas feeding system; (iii) Gas mixer; (iv) Gas mixture ignition system; and (v) Data acquisition system.

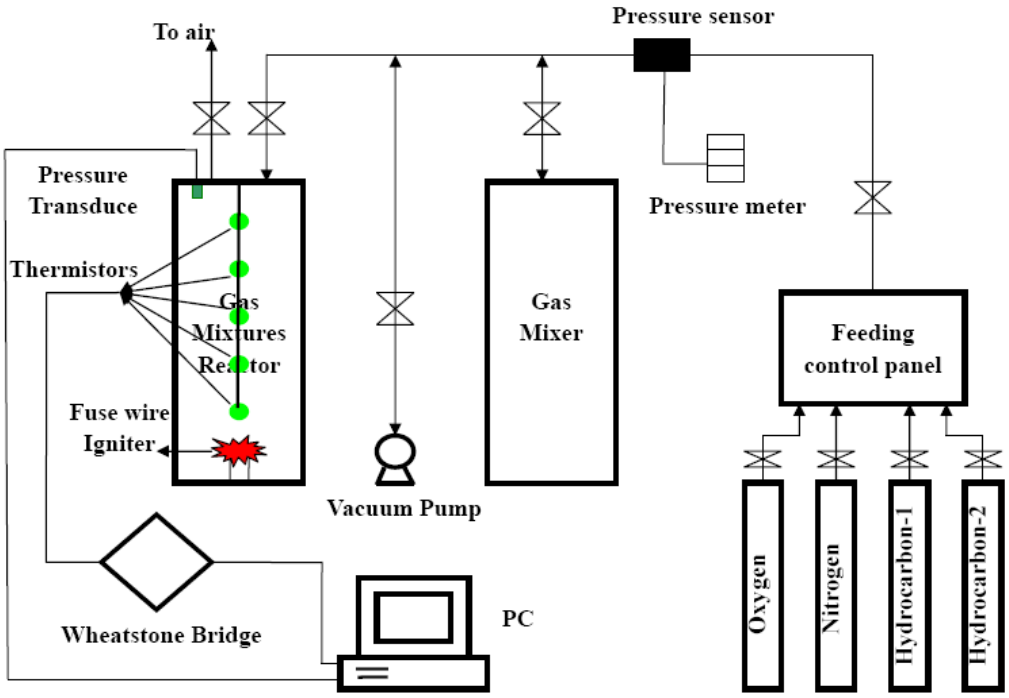


Fig. 3.1. Schematic representation of experimental apparatus.

### 3.2.1 Reaction Vessel

The reaction vessel (Figure 3.2) is a closed cylinder with diameter 4 inch nominal (11.43 cm O.D., 10.22 cm I.D.) and length 100 cm. It hangs from a top plate permanently affixed to the vessel enclosure. At the central line of the reaction vessel, there are five evenly-separated temperature sensors consisting of NTC thermistors (Thermometrics, FP07DB104N with fast response time 0.1 sec in still air and 100 KΩ resistance at 25$^{o}$ C), which can detect frame front in real time and locate self-sustained frame propagation distance when fuel/air mixtures ignite and burn upwardly. The greatest distance from the ignition source to thermistor 5 is 75 cm. This design is

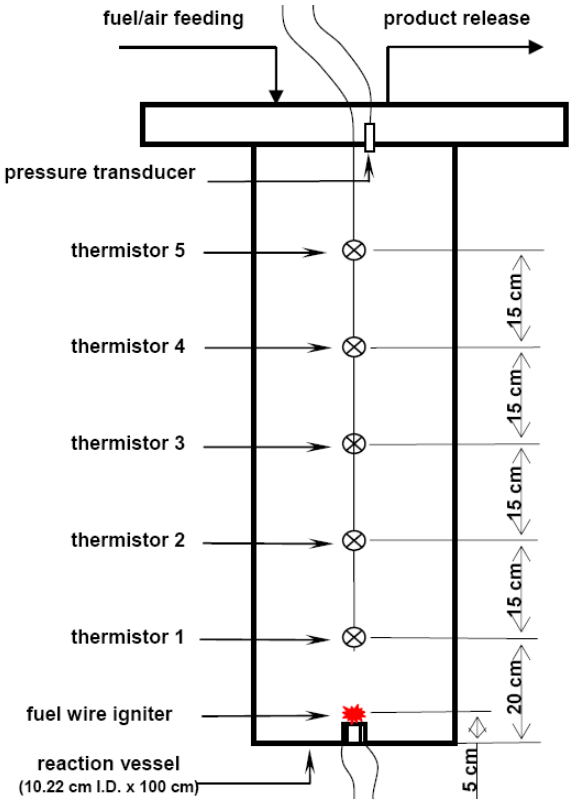


Fig. 3.2. Configuration of reaction vessel.

is consistent with the flammability apparatus of Bureau of Mines when using visual observation as a flammability limit detection criterion [13]. Thermistor 1 is located at the distance of 15 cm away from the ignition source (at the bottom of reaction vessel), which can effectively lower the heat impact from the ignition source. At the top of reaction vessel, there is a dynamic pressure transducer (Omega DPX 101, with a range of 0 to 250 psig pressure rise, 0 to 5 V nominal output signal, 1 μs rise time, 1% amplitude linearity and temperature effect of 0.03%/F) is mounted on the top plate and used to record the pressure variation when fuel/air mixtures ignite or explode. Britton [12] recommended this geometry partly for ease of maintenance, but mostly because

when combined with bottom ignition the pressure rise will be relatively large so that a pressure criterion can easily be applied. The geometry is also similar to that of the apparatus used by the Bureau of Mines and the more recent European standard EN 1389 (T). Previous work has shown that reaction vessels with similar dimension have sufficient width to minimize quenching of typical fuel flames and sufficient distance between the igniter and pressure sensor at the top of the vessel to minimize ignition energy effects on the measurement results [45].

3.2.2. Gas Feeding System

The gas feeding system includes a manifold that connects to the chemical cylinders, a vacuum pump (Welch Mfg. Duoseal Pump with ultimate vacuum $1.0x10^{-3}$ mmHg), the mixing vessel, and a reaction vessel. The gas mixtures used with the experimental apparatus are synthesized by loading the individual components from the pressurized cylinders in which they are supplied into an external mixing device through a gas feeding manifold (Figure 3.3). The combined gas line from all pressurized cylinders leads to a cross junction, which includes a pressure transducer (Omega PX603, 0.4% accuracy with 0.04%/F thermal zero and span effect) connected with a pressure meter. Mixture composition was controlled through partial pressure gauging recommended by Bureau of Mines [22]. Theoretically, at external conditions of room temperature and ambient pressure, the calculated compressibility factor is very close to 1, which means the fuel/air mixtures at standard conditions can be treated as ideal gas mixtures.

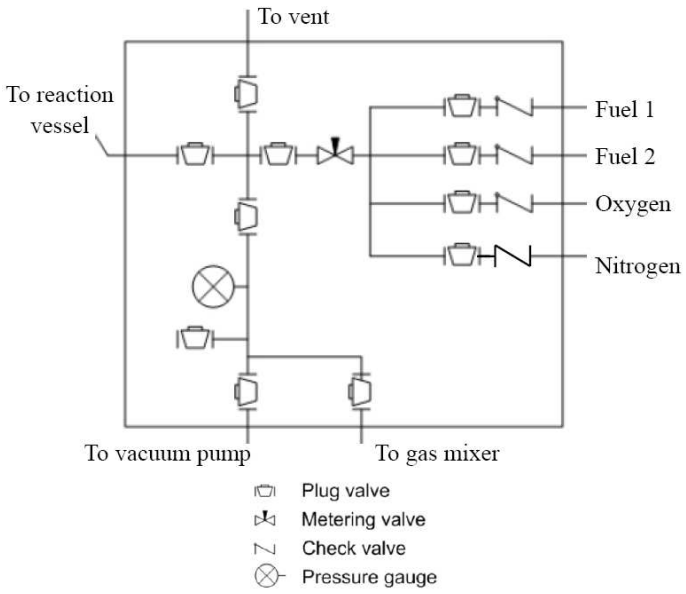


Fig. 3.3. Gas feeding manifold.

### 3.2.3 Gas Mixer

Premixed fuel/air mixtures are employed in this research to measure the flammability limit. The feeding gas mixtures are made to be homogeneous using a gas mixer which is a cylinder containing a cylindrical Teflon block. This block can slide along the length of the vessel, and the block diameter is slightly smaller than the gas mixer's internal diameter, which allows smooth movement of the block. Gas mixing is obtained by rotating the mixer. Gases moving between the block and the vessel wall create highly turbulent zones in front of and behind the moving block, and these zones facilitate fast mixing of the gases. The volume of gas mixer approximates the volume of the reaction vessel, which ensures precise gauging of feeding components through partial pressures (not small volumes), easy handling, and cost effectiveness (not big volume).

### 3.2.4 Gas Mixture Ignition System

The gas mixture igniter system used in this research is similar to that outlined in ASTM E 918-83, which was demonstrated by Mashuga to be capable of inputting 10 J of energy with a repeatable power delivery [35]. The ignition source is a 10 mm piece of AWG 40 tinned copper wire, which is vaporized by a 500 VA isolation transformer (Hammond 171 E) at 115 V AC switched on with a zero-crossing solid state relay (Omega, model #SSRL240DC 100), and the current is delivered beginning at the zero point of each AC cycle.

### 3.2.5 Data Acquisition System

In this research, five NTC thermistors and one dynamic pressure transducer are used to detect combustion and record temperature and pressure changes in the reaction vessel. Of five thermistors, each is the resistance to be measured ($R_T$) in a Wheatstone bridge circuit consisting of three other resistors with constant resistance ($R_1$, $R_2$, $R_3$), as shown in Figure 3.4. The advantage of five parallel Wheatstone bridge circuits is that, unlike resistance, the voltage difference can be measured directly and converted to resistance values as long as the values of three constant resistors are known. In this case the bridges are initially balanced with each $V_{out}$ equal to zero. When any one of the thermistors detects a flame, the related bridge deviates from the balance and a nonzero $V_{out}$ value indicates the temperature change at the position of this thermistor. For the purpose of flame detection rather than flame temperature determination, calculation of the temperature is not necessary as passage of a flame will induce sharp increases in the

voltage signal because the temperature trends of the gas mixture during and after combustion can be observed.

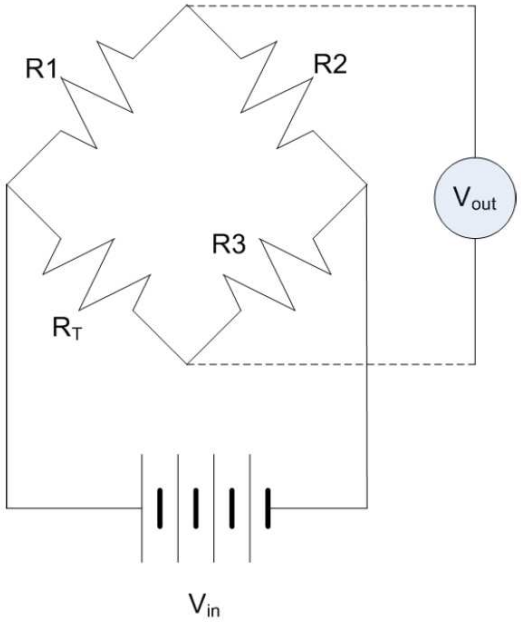


Fig. 3.4. Wheatstone bridge circuit used for flame detection.

Data acquisition is performed with a desktop computer equipped with a Keithley data acquisition card (Keithley KPCI-3102, 8 differential inputs with total of 225 signals per second @0.05% accuracy) with screw terminal attachment (Keithley, STP-68). The data acquisition card measures differential voltages, allowing it to measure both the thermistors and the pressure transducer. The measurement process is controlled by a LabView® program (National Instruments, version 7.1).

### 3.3 Detection Criterion for Flammability Limit Measurement

This work uses an innovative thermal criterion for flammability determination based on Wong's research [46]. In the closed reaction vessel, five NTC thermistors at multiple locations are employed to track flame propagation, which indicates the sensitive thermistors can locate the flame traveling distance from the ignition source in real time. Bureau of Mines used a certain flame propagation distance (equal to half of reaction tube length with150 cm total) as the detection criterion by visual observation, in which the working mechanism is similar to the thermal criterion using thermistors to detect flame propagation instead of naked eyes. Meanwhile, the new thermal criterion is connected to a relative pressure rise criterion that is well standardized by ASTM E 2079. A dynamic pressure transducer lying on the top of reaction vessel can record the dynamic pressure change in the reaction vessel to confirm the occurrence of fire or an explosion in the reaction vessel. Specifically, the maximum pressure is obtained by integrating the portion of the dynamic pressure *vs.* time curve that is above the baseline, and applying a conversion factor of 51.02 psi per V•sec (from the manufacturer specification).

### 3.4 Experimental Procedures

A flammability experiment is a systematic operation, which includes a series of actions: (i) Evacuation of the gas mixer, reaction vessel and tubing lines; (ii) Gas loading; (iii) Mixing of feeding gases; (iv) Premixed fuel/air mixture transfer; (v) Premixed fuel/air mixture ignition; and (vi) Flammability data acquisition. Because the original objective for this research is to find the critical fuel concentrations as LFLs or UFLs, all the operations should follow the proper sequences for accurately gauging

feeding gases, especially at the stage of controlling plug valves (Figure 3.5). Following is the step-by-step operation procedure for one entire experiment.

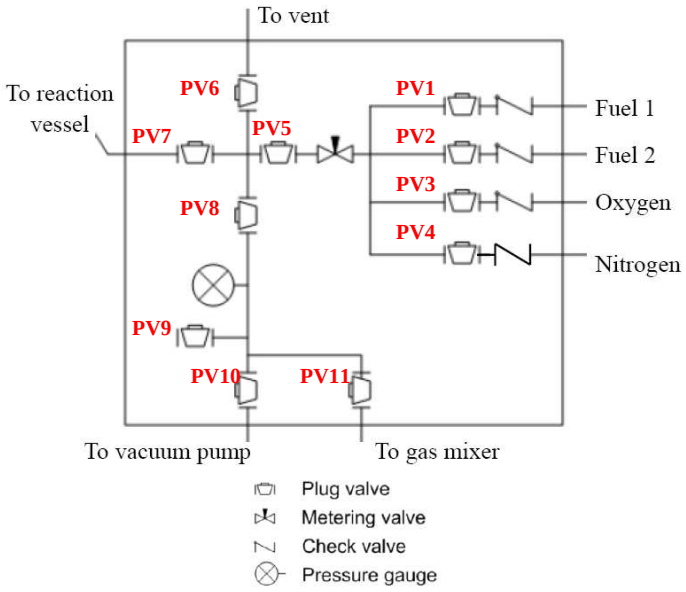


Fig. 3.5 Gas feeding manifold and marked controlling plug valves.

Step 1: Preparation for gas feeding. The vacuum pump is activated to evacuate the reaction vessel (PV7, PV8, PV10 open; all other plug valves closed), mixing vessel (PV8, PV10, PV 11 open; all other plug valves closed) and gas loading manifold (PV1, PV2, PV3, PV4, PV5, PV8, PV10 open; all other plug valves closed) until the pressure is constant for over one minute (pressure change no greater than 0.01 psi). The pressure is recorded for gas mixture composition calculations on an Excel spreadsheet.

Step 2: Loading gases one by one. Fuel 1 is loaded first (PV1, PV5, PV8, PV11 open; all other plug valves closed), followed by Fuel 2 (PV2, PV5, PV8, PV11 open; all other plug valves closed), nitrogen (PV3, PV5, PV8, PV11 open; all other plug valves

closed) and oxygen (PV4, PV5, PV8, PV11 open; all other plug valves closed). The gas loading manifold is evacuated between every component loading (PV5, PV8, PV10 open; all other plug valves closed). The loading amounts are controlled by the predetermined pressure values gauged by a pressure meter. The final pressure is recorded on the Excel spreadsheet to convert into the gas mixture volume concentrations.

Step 3: Mixing the feeding gas mixtures. The external mixer is utilized after the gas loading is complete. Care should taken to ensure the plug valve on the top of the mixing vessel is closed, the manifold opened to the ventilation (PV5, PV8, PV10 open; all other plug valves closed). After disconnection with the manifold, start the rotation motor with slowly increasing voltage to the pre-set value (30 rounds per min). The motor is de-activated after 5 minutes, and the mixing vessel is reconnected to the manifold.

Step 4: Loading premixed fuel/air mixtures into reaction vessel. The tubing line between the mixing vessel and the manifold must be vacuumed before premixed fuel/air is transferred to the reaction vessel (PV8, PV10, PV11 open; all other plug valves closed). Once the reaction vessel has filled to one atmosphere pressure (14.7 psi), it is isolated from the manifold by closing PV7. The gas mixtures are allowed to sit in the reaction vessel for five minutes to reach thermal equilibrium and become quiescent. At the same time, the inert plug valve PV4 is opened to add the inert gas nitrogen to lower the fuel concentration in the manifold and the mixing vessel until it is no longer combustible.

Step 5: Gas mixture ignition and data acquisition. Before this operation is begun, the LabView is activated to begin recording. Approximately 5 sec after the data acquisition starts, the gas mixture is ignited by a fuse wire igniter, and the program LabView continues running to record the flame temperature until the premixed fuel/air mixture is consumed by traveling to the top of reaction vessel. The ignition and subsequent combustion can be detected by thermistor and pressure transducer readings for a period of time ~17 s. The readings are voltage values with 2,000 data points for each sensor (5 thermistors and 1 pressure transducer).

Step 6: The flammability apparatus is prepared and the experiment is repeated with the same steps as above.

# CHAPTER IV

# EXPERIMENTAL RESULTS AND DATA ANALYSIS

## 4.1 Overview

The flammability limits (LFL and UFL) of binary hydrocarbon mixtures in air were measured in this research by using the thermal criterion developed for this apparatus. The results of flammability limits for binary hydrocarbon mixtures were obtained at standard conditions (room temperature and ambient atmospheric pressure) with upward propagation. The experimentally determined flammability limits for pure hydrocarbons are compared with existing data reported in the literature serving as experimental calibration. Predictions using Le Chatelier's Law were fit to all experimental data (LFLs and UFLs) for various two-component combinations from saturated and unsaturated hydrocarbons (methane, ethylene, propylene, n-butane, acetylene). Modification of this law was used if experimental observations showed large deviations from Le Chatelier's predictions. Meanwhile, experimentally measured flammability limit data were analytically related to the stoichiometric concentrations for different binary hydrocarbon mixtures.

## 4.2 Combustion Types in Reaction Vessel

Combustion behavior in reaction vessel was classified into five categories over a range of concentrations that span from below the lower flammability limits to above the upper flammability limits for fuel/air mixtures: (i) Non-propagation; (ii) Flash combustion; (iii) Discontinuous flame propagation; (iv) Temperately continuous flame

propagation; and (v) Violently continuous flame propagation. The sampling experiments were conducted with methane/air and ethylene/air mixtures. The data from thermal and pressure sensors were acquired and interpreted to identify the combustion types. The thermal criterion was developed for the flammability apparatus by matching combustion behaviors with the signal *vs.* time curves of sensors.

### 4.2.1 Non-propagation Combustion

Non-propagation combustion is characterized by the property of lacking flame propagation after ignition, which can be due to a variety of factors, such as very low fuel or oxidizer concentrations, low ignition energy input or low ignition energy density [46]. In this experiment, the ignition energy was applicable to fire fuel/air mixtures. Under proper working conditions, therefore, the occurrence of non-propagation combustion would originate from relatively lean fuel concentrations in air. Figure 4.1 shows the temperature and pressure profiles for non-propagation combustion (not a direct relationship between time and temperature or pressure, while the voltage can reflect the variation tendency of temperature and pressure with time in the reaction vessel). Generally, non-propagation behavior in the flammability apparatus has no or negligible temperature and pressure fluctuations. Sometimes, a small temperature spike would come from a portion of the fuel/air mixture heated by the ignition energy and rising to the nearest thermistor's area. The temperature quickly cooled down because of heat loss to surroundings, thus no change in temperature is indicated by the thermistors farther from the ignition source.

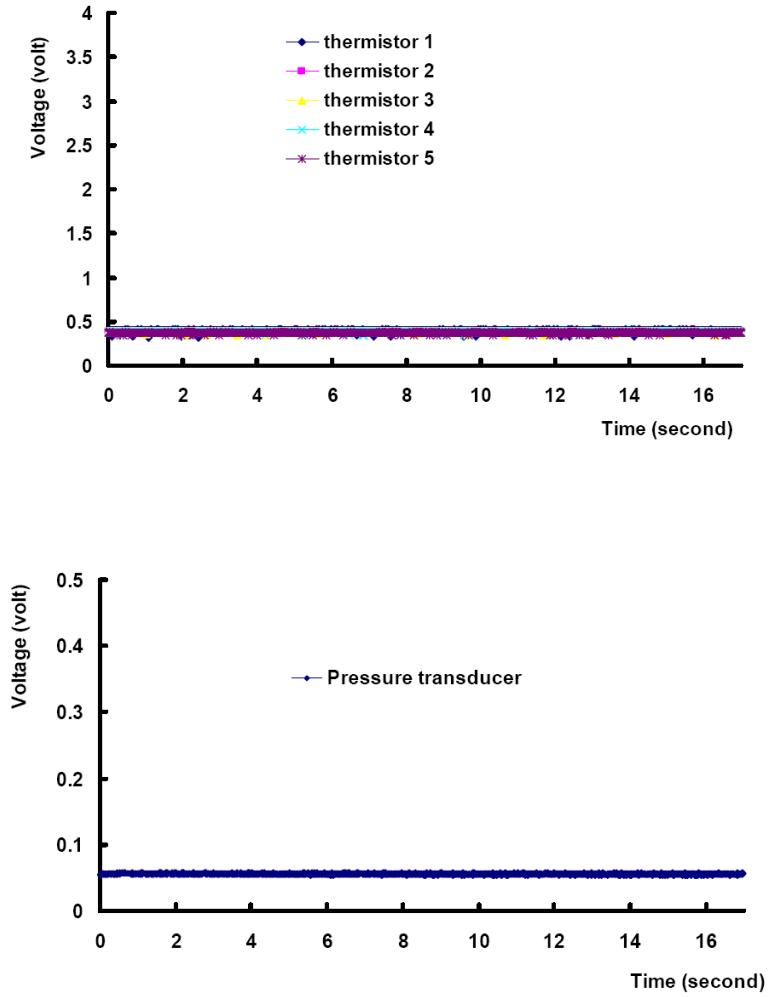


Fig. 4.1. Temperature (top) and pressure (bottom) profiles for non-propagation combustion.

4.2.2 Flash Combustion

Flash combustion is flame with vertical flame propagation, but little or no horizontal propagation, which terminates within a short distance of the ignition source to produce minor temperature and pressure increases [46]. Figure 4.2 shows the temperature and pressure data for the flash combustion of 4.35% methane in air at 25 ºC and 14.7 psi.

The flash combustion example shows only that the very lower part of methane/air mixture in reaction vessel combusted, and the flame terminated before it reached to the position of thermistor 1 (the peak temperature value indicated by a peak voltage of about 2.5 volts, while the predicted maximum value was about 3.5 volts when the flame front reached this position). The reasonable explanation is that a combusting fuel/air mixture will travel upward because of buoyancy force, and due to heat loss its temperature will decrease continuously until it drops to ambient temperature of fuel/air mixture. In this case, flash combustion has a minor temperature and pressure increases.

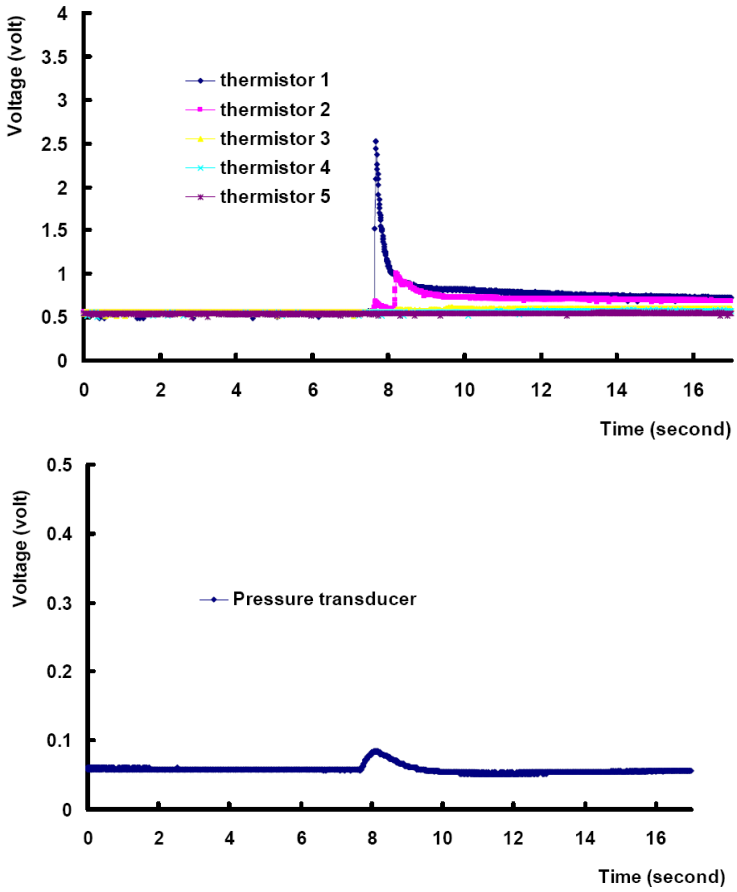


Fig. 4.2. Temperature (top) and pressure (bottom) profiles for flash combustion.

4.2.3 Discontinuous Flame Propagation

Discontinuous flame propagation is a flame that propagates vertically and horizontally but terminates before reaching the top of the reaction vessel. The temperature and pressure profiles of discontinuous flame propagation illustrated in Figure 4.3 differ substantially from the profiles of flash combustion. The flame could propagate almost to the location of thermistor 3 (Thermistor 1, thermistor 2 and

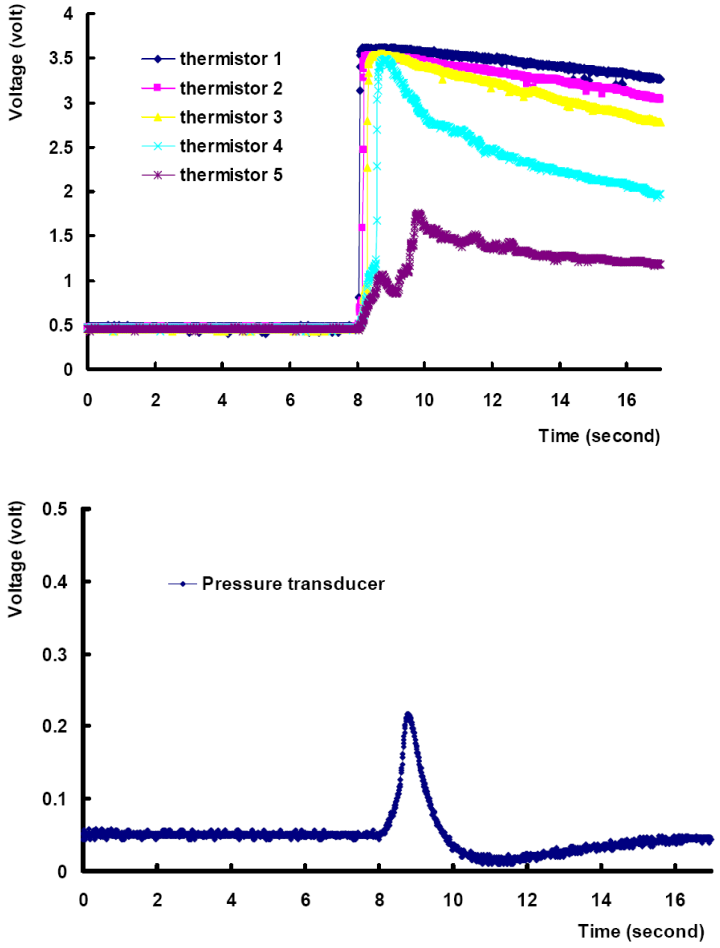


Fig. 4.3. Temperature (top) and pressure (bottom) profiles for discontinuous flame propagation.

thermistor 3 have similar signal profiles, which indicates that the flame front could pass through all of them; however, themistor 4 and thermistor 5 have inconsistent profiles with thermistor 1, thermistor 2, thermistor 3, because thermistor 4 and thermistor 5 are detecting hot gases rising from below instead of flame propagation past them). The maximum pressure is significantly greater than the pressure rise caused by flash combustion, because a greater portion of the gas in the reaction vessel participates in combustion than in the flash combustion behavior.

### 4.2.4 Temperately Continuous Flame Propagation

Temperately continuous flame propagation occurs when the flame is able to propagate vertically and horizontally and does not terminate until it reaches the top of the reaction vessel. In this case, all the thermistors detect the flame front in succession and then slowly decrease as the gas around the thermistors cools, so they exhibit similar temperature profiles. Comparing with flash combustion and discontinuous flame propagation, a greater pressure rise is obtained, which illustrates more gas is combusted in the experiment. Of five combustion types, temperately continuous flame propagation is the result we seek after with tests of different fuel concentrations, because the fuel concentrations marked in this combustion type are used to determine the lower and upper flammability limits of fuel/air mixtures.

Figure 4.4 shows temperature and pressure measurements from the combustion of 5.25% methane in air, in which the fuel/air mixture ignited and the flame propagated to the top of reaction vessel exactly. The pressure measurements indicate a maximum

pressure about 17 psi (115 % rise), which is much larger than the pressure rise criterion specified by the ASTM methods (7%) or the criterion specified by En 1839(B) (5%).

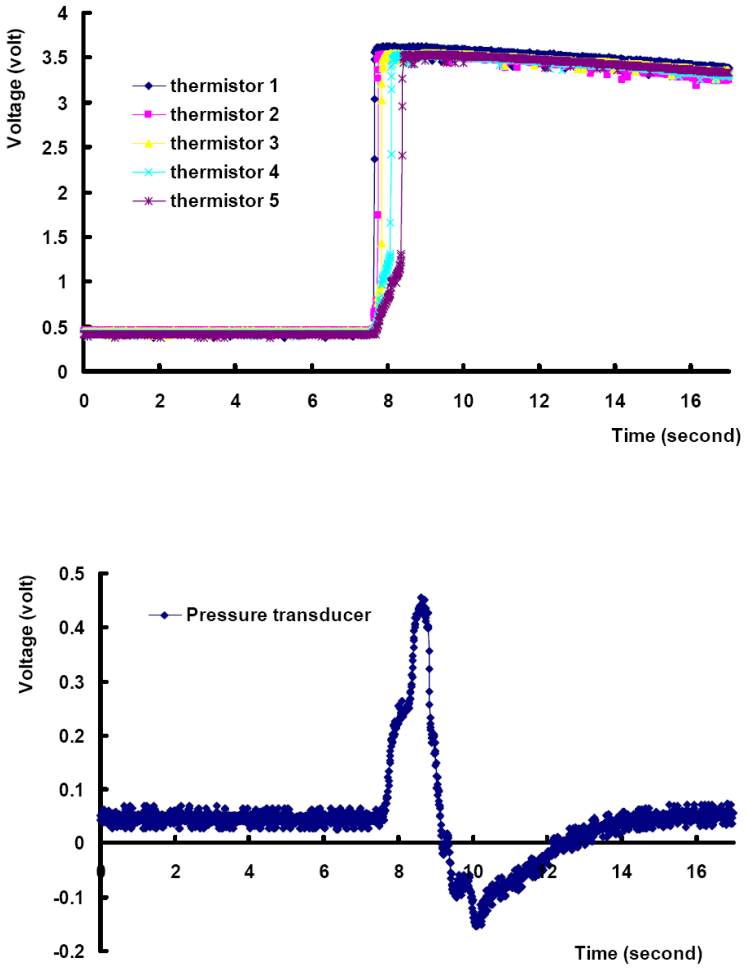


Fig. 4.4. Temperature (top) and pressure (bottom) profiles for temperately continuous flame propagation.

### 4.2.5 Violently Continuous Flame Propagation

Violently continuous flame propagation describes that a fuel/air mixture in reaction vessel combusts violently, the flame propagates upward and dynamic pressure varies much more rapidly than the temperately continuous flame propagation. Figure 4.5 represents the temperature and pressure profile of violently continuous flame

propagation with the stoichiometric concentration of ethylene in air (6.53%) at ambient conditions. The experimental result indicates that at this fuel concentration ethylene combusted violently, which is consistent with the principle that fuel/air combustion rate will change with the molar ratio of fuel to air, and the maximum value lies near the stoichiometric concentration.

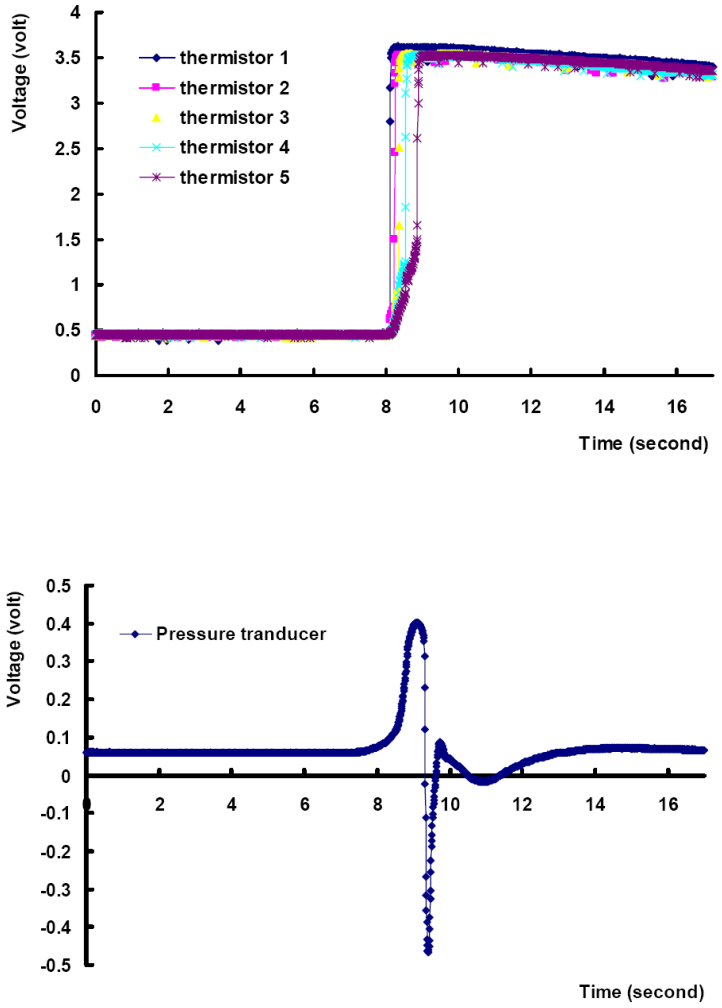


Fig. 4.5. Temperature (top) and pressure (bottom) profiles for violently continuous flame propagation.

### 4.3 Calibration for Flammability Limits Estimation

Nearly two hundred years of research on flammability has produced a variety of measurement methods. Even though different detection criteria and apparatus setups are applied in these methods, the key point, however, was similar, such as, flame propagation to a certain distance from the ignition source. In this research, a thermal criterion was introduced, where five thermistors were used to detect the flame front location in the reaction vessel, and a dynamic pressure transducer was employed to record the relative pressure rise. Based on the information of five different combustion types, fuel concentrations could be characterized by temperature and pressure profiles. When continuously increasing fuel concentrations, we observed that flame traveled farther up to the top of reaction vessel. Figure 4.6 is an example illustrating flame propagation distance variation with different concentrations of methane in air.

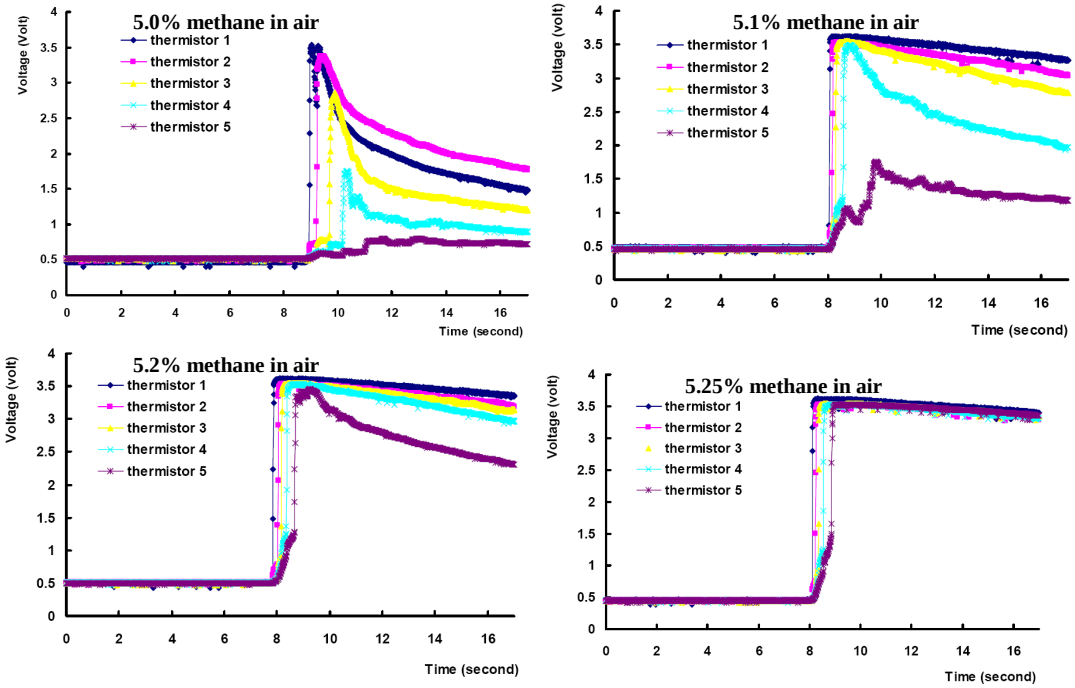


Fig. 4.6. Flame propagation profiles with different methane concentrations in air.

Common practice, recommended by ASTM methods [26], is to determine the lower flammability limit by averaging the lowest fuel concentration with flame propagation and the highest concentration in which flame will not propagate, and *vice versa* for the upper flammability limit. Wierzba et al. [47] showed that probability of flame propagation can vary from 0 to 100% when the fuel is within a certain concentration range near the flammability limits. Based on the ideas from the definition and probability property of flammability, in this research, a series of experiments were conducted to measure the probability of continuous flame propagation at a certain concentration (near the flammability limits) for a fuel/air mixture, and the same operations were repeated at different concentrations. The propagation probabilities were plotted against different fuel concentrations, and by regression a linear function was obtained, where a concentration with 50% of probability of continuous flame propagation was identified as the LFL or UFL of the fuel at these experimental conditions.

For calibration purposes, the original experiments for flammability limit determination were performed using pure hydrocarbons: methane and ethylene. Table 4.1 shows the probability of continuous flame propagation at different percentage concentrations of methane in air, where for every concentration the measurement was repeated ten times, and the result of continuous flame propagation was recorded. Figure 4.7 provides a graphical representation of data presented in Table 4.1, and LFL of methane in air at standard conditions was obtained by finding the concentration point

with 50% probability of continuous flame propagation. The same procedure was used to determine the LFL of ethylene in air at standard conditions (Table 4.2 and Figure 4.8).

Table 4.1 Probabilities of continuous flame propagation at different concentrations of methane in air.

| Methane Conc. (molar %)* | Measurement times | Continuous Flame Propagation times | Probability of Continuous Propagation |
|---|---|---|---|
| 5.22 | 10 | 0 | 0% |
| 5.23 | 10 | 2 | 20% |
| 5.24 | 10 | 4 | 40% |
| 5.25 | 10 | 4 | 40% |
| 5.26 | 10 | 7 | 70% |
| 5.27 | 10 | 7 | 70% |
| 5.28 | 10 | 8 | 80% |
| 5.29 | 10 | 10 | 100% |

* @ room temperature (25 °C) and 1 atmospheric pressure

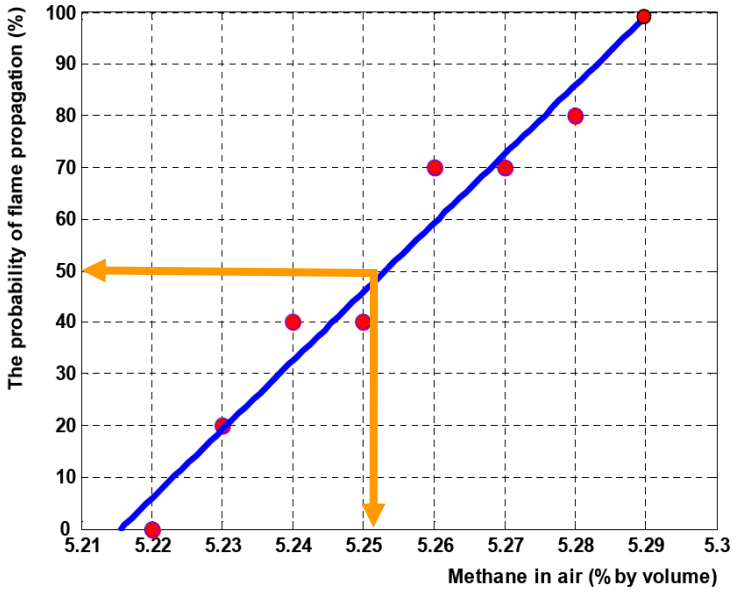


Fig. 4.7. Determination of LFL of methane in air using thermal criterion.

Table 4.2 Probabilities of continuous flame propagation at different concentrations of ethylene in air.

| Ethylene Conc. (molar %)* | Measurement times | Continuous Flame Propagation times | Probability of Continuous Propagation |
|---|---|---|---|
| 2.78 | 10 | 0 | 0% |
| 2.79 | 10 | 2 | 20% |
| 2.80 | 10 | 4 | 40% |
| 2.81 | 10 | 6 | 60% |
| 2.82 | 10 | 7 | 70% |
| 2.83 | 10 | 7 | 70% |
| 2.84 | 10 | 10 | 100% |

* @ room temperature (25 °C) and 1 atmospheric pressure

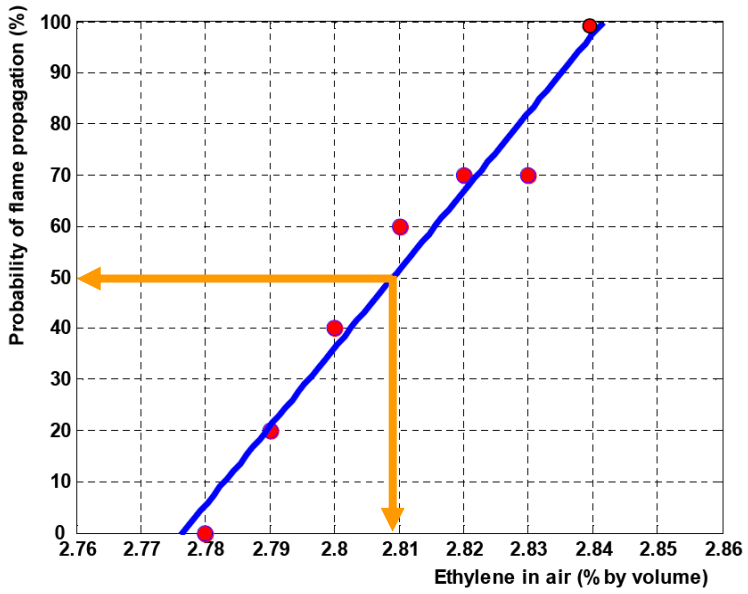


Fig. 4.8. Determination of LFL of ethylene in air using thermal criterion.

Using this thermal criterion, the experimentally determined LFLs of pure methane and pure ethylene were compared with some literature data from previous

research with different experimental setups and detection criteria, and the data are shown in Table 4.3 (methane) and Table 4.4 (ethylene). The experimental data from this research slightly differ from previous measurements, but these deviations are reasonable and acceptable because flammability changes with experimental configurations and detection criteria.

Table 4.3 Low flammability limits of methane in air (25 ºC and 1 atm)

| Methane LFL in Air | Apparatus types |
|---|---|
| **5.3%** | Vertical glass cylinder |
| **4.85%** | 20 L sphere, 7% pressure rise |
| **4.3%** | EN 1839 (T) |
| **4.95%** | EN 1839 (B) |
| **4.66%** | Counterflow burner |
| **5.23%** | Wun Wong's Experiment |
| **5.25%** | My experiment |

Table 4.4 Low flammability limits of ethylene in air ((25 ºC and 1 atm)

| Ethylene LFL in Air | Apparatus types |
|---|---|
| **3.05%** | Vertical glass cylinder |
| **2.62%** | 20 L sphere, 7% pressure rise |
| **2.4%** | EN 1839 (T) |
| **2.6%** | EN 1839 (B) |
| **2.71%** | Wun Wong's Experiment |
| **2.81%** | My experiment |

### 4.4 LFLs and UFLs of Binary Hydrocarbon Mixtures

The binary hydrocarbon mixtures that were measured consist of the combinations of some typical hydrocarbons including saturated alkanes (methane and n-butane),

double-bonded unsaturated alkenes (ethylene and propylene), and one triple-bonded unsaturated alkyne (acetylene). The flammability limits (LFLs and UFLs) of binary hydrocarbon mixtures were determined in air at atmospheric pressure (14.7 psi) and room temperature (25 $^{o}$C) using the thermal criterion. Specifically, the LFLs and UFLs of methane and n-butane, methane and ethylene, methane and acetylene, and ethylene and propylene were measured. At the same time, the related uncertainties in the experiments were considered, where the uncertainties originated from random errors (gas feeding errors and gauging errors) and the contribution from system errors were neglected. The uncertainty for flammability estimation was calculated using the principle of error propagation, and the magnitude of uncertainty was indicated by error bars.

### 4.4.1 LFLs of Binary Hydrocarbon Mixtures

The experimentally measured lower flammability limits of methane and n-butane, methane and ethylene, methane and acetylene, ethylene and propylene, and ethylene and acetylene are presented in Figure 4.9 – 4.13, respectively, in which the theoretically calculated lower flammability limits were plotted as well by applying Le Chatelier's Law. By comparing the experimental observations with the predictions from Le Chatelier's Law, we could easily find that the experimental data (lower flammability limits in air at standard conditions) were fit very well by Le Chatelier's Law. The result is consistent with deviation of Le Chatelier's Law conducted by Mashuga and Crowl [44], because at the lower flammability limit condition, almost all the hydrocarbon mixtures can be approximated to the assumption requirements for the derivation of Le Chatelier's Law.

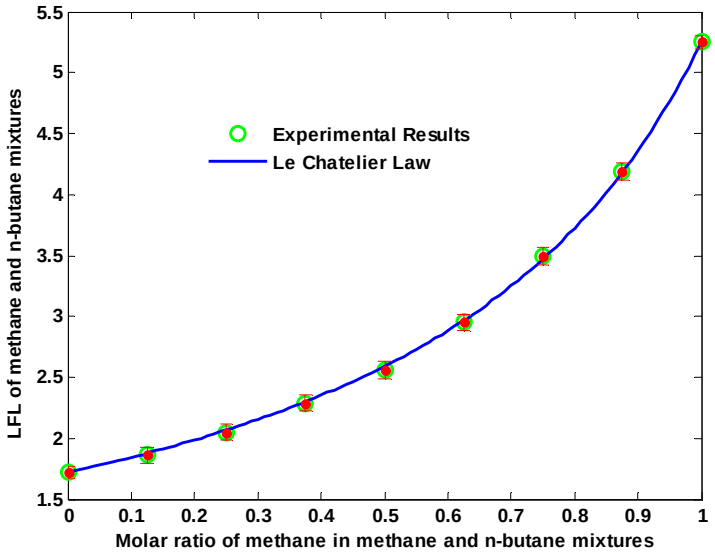


Fig. 4.9. Lower flammability limits of methane and n-butane mixtures in air at standard conditions.

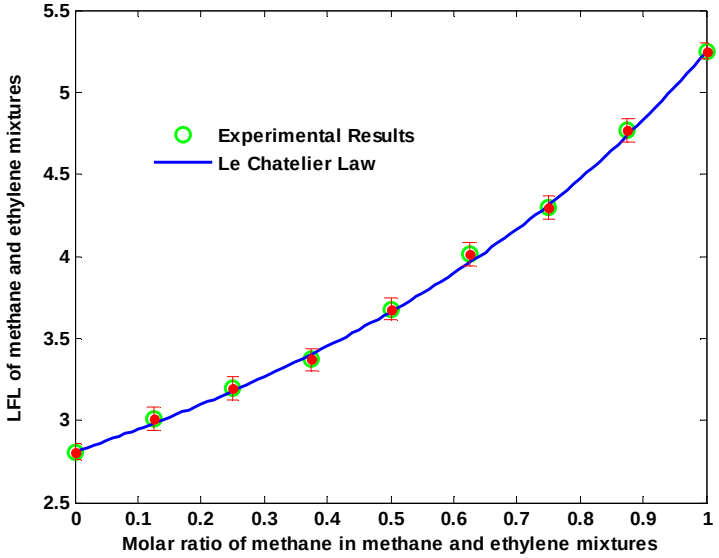


Fig. 4.10. Lower flammability limits of methane and ethylene mixtures in air at standard conditions.

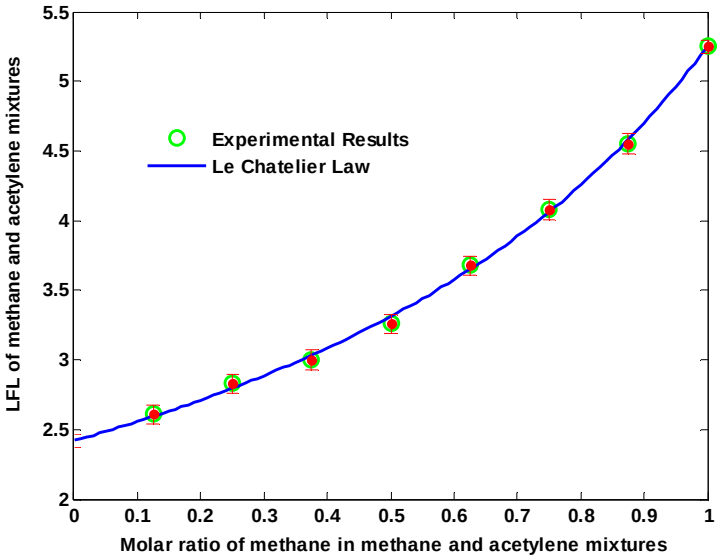


Fig. 4.11. Lower flammability limits of methane and acetylene mixtures in air at standard conditions.

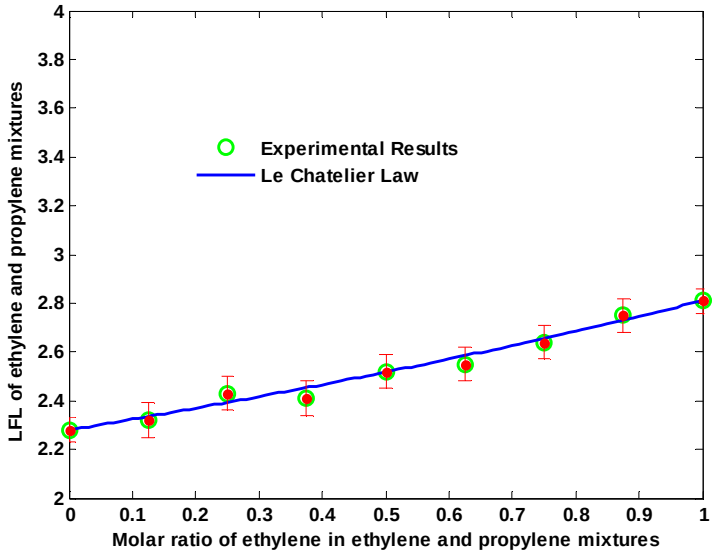


Fig. 4.12. Lower flammability limits of ethylene and propylene mixtures in air at standard conditions.

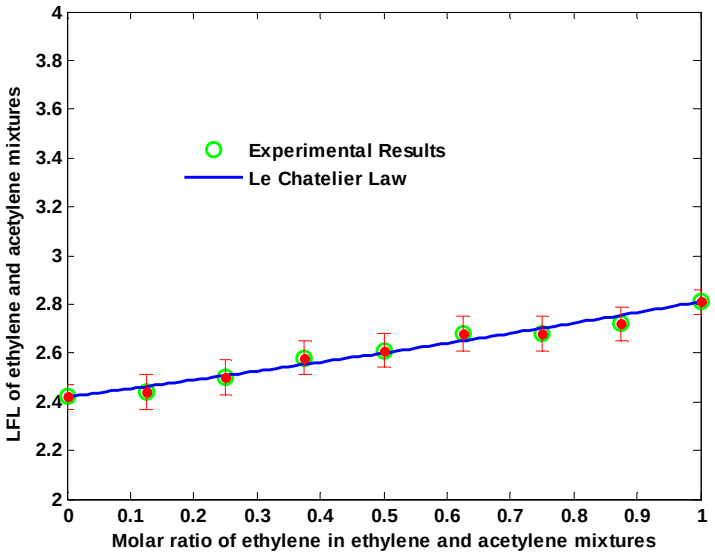


Fig. 4.13. Lower flammability limits of ethylene and acetylene mixtures in air at standard conditions.

4.4.2 UFLs of Binary Hydrocarbon Mixtures

Figure 4.14 - 4.18 show the upper flammability limits of methane and n-butane mixtures, methane and ethylene mixtures, methane and acetylene mixtures, ethylene and propylene mixtures, and ethylene and acetylene mixtures at different volumetric ratios, respectively. As with the lower flammability limits of these hydrocarbon combinations, the experimental observations are compared with calculations using Le Chatelier's Law, in which Le Chatelier's Law can roughly fit the UFL data of methane and n-butane, the measured UFLs of methane and ethylene mixtures, ethylene and propylene mixtures, ethylene and acetylene mixtures deviated from Le Chatelier's predictions moderately, while the UFL data of methane and acetylene exhibited a big gap with predictions from Le Chatelier's Law.

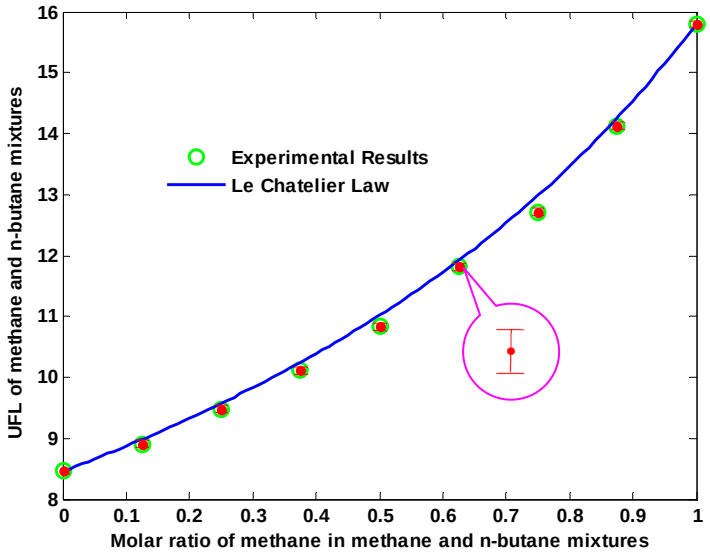


Fig. 4.14. Upper flammability limits of methane and n-butane mixtures in air at standard conditions.

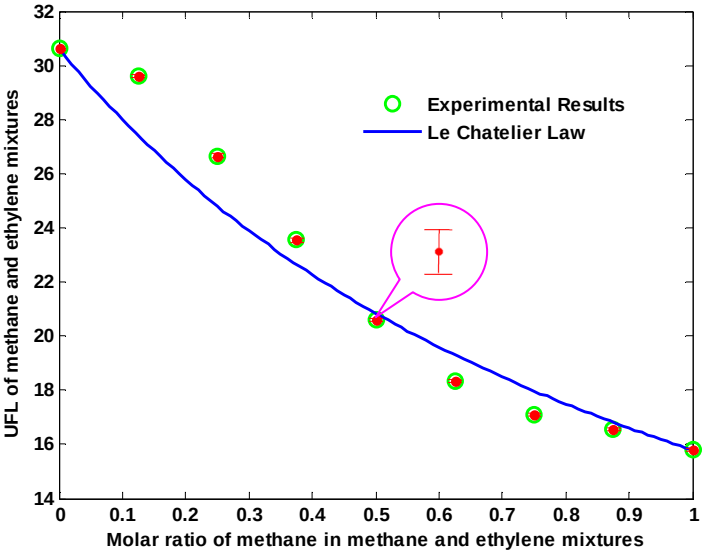


Fig. 4.15. Upper flammability limits of methane and ethylene mixtures in air at standard conditions.

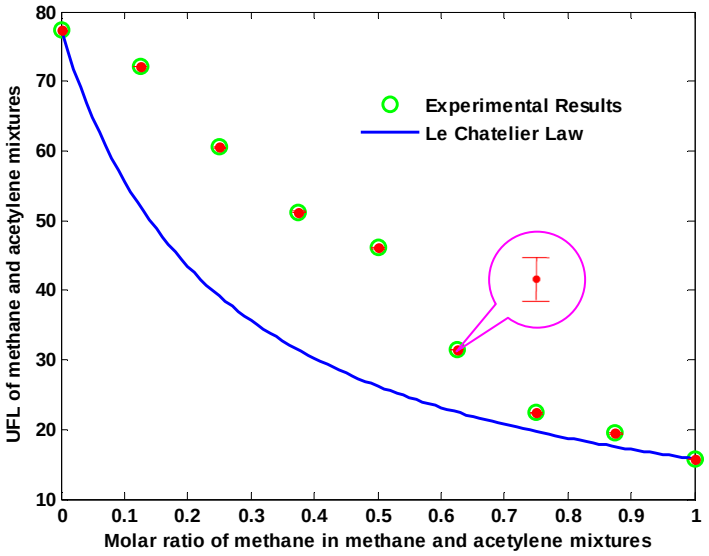


Fig. 4.16. Upper flammability limits of methane and acetylene mixtures in air at standard conditions.

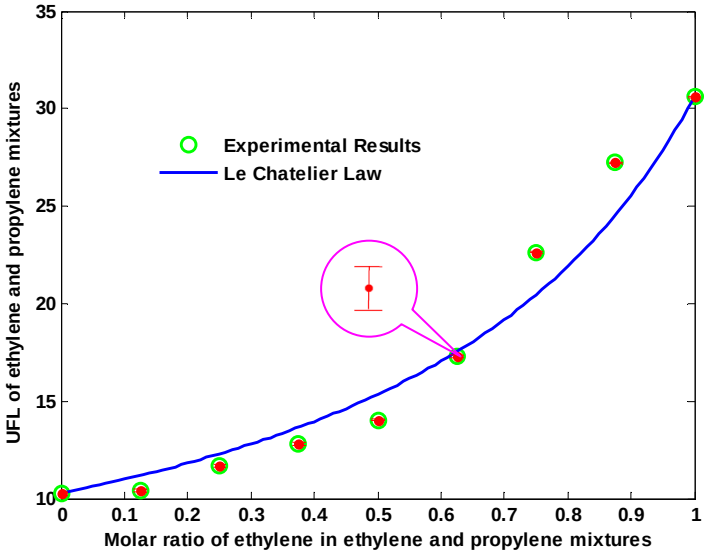


Fig. 4.17. Upper flammability limits of ethylene and propylene mixtures in air at standard conditions.

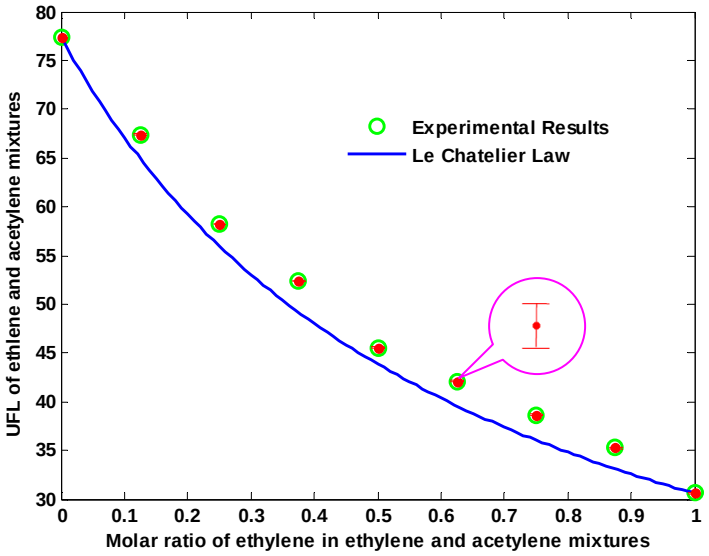


Fig. 4.18. Upper flammability limits of ethylene and acetylene mixtures in air at standard conditions.

## 4.5 Numerical Analyses of Experimentally Measured Flammability Limit Data

In this section, results of numerical analyses conducted on the measured flammability limit data (LFLs and UFLs) are shown for quantitative characterization of flammability limits of binary hydrocarbon mixtures, which include the modification of Le Chatelier' Law and relating LFLs or UFLs to the stoichiometric concentrations of fuel mixtures in air.

### 4.5.1 Modification of Le Chetalier's Law

Le Chetalier's Law is still popularly used for its simplicity and effectiveness to estimate the flammability limits of fuel mixtures. Its accuracy, however, becomes low or unacceptable when applied to predict upper flammability limits of fuel mixtures. Because Le Chatelier's law is an empirically summarized formula which originated from the evaluation of mixing flammability at lower fuel concentrations (LFLs), its extended

application at higher fuel concentrations (UFLs) was only limited to some fuel mixtures [43]. Mashuga and Crowl [44] developed a theoretical derivation for this law with several pre-required assumptions. At lower fuel concentrations, these assumptions are consistent with real situations, which means Le Chatelier's Law can be theoretically confirmed to estimate LFLs of fuel mixtures; while at concentrations of upper flammability limits, these assumptions will deviate from real conditions, which result in the application limits for this law. The experimental data from this research also shows the same results as stated above when Le Chatelier's Law is fit to the data: (i) Le Chatelier's Law can be confidently used to estimate the lower flammability limits of binary hydrocarbon mixtures; (ii) For acceptable accuracy, modification of Le Chatelier's Law is required when used to predict upper flammability limits, where the binary hydrocarbon mixtures contain unsaturated hydrocarbons (double-bonded and triple-bonded components).

**Methane and n-butane mixtures:** Table 4.5 shows the experimental data and their absolute and relative deviations from the predictions of Le Chatelier's Law for the lower and upper flammability limits of methane and n-butane mixtures. The relatively smaller deviations indicate Le Chatelier's formula (Eq. (26), Eq. (27)) can be directly used to calculate the lower and upper flammability limits of methane and n-butane mixtures.

$$\frac{1}{LFL_{methana/n-butane}} = \frac{x}{LFL_{methane}} + \frac{1-x}{LFL_{n-butane}} \tag{26}$$

$$\frac{1}{UFL_{methana/n-butane}} = \frac{x}{UFL_{methane}} + \frac{1-x}{UFL_{n-butane}} \tag{27}$$

Table 4.5 Flammability limit data from experimental measurements and Le Chatelier's Law (methane and n-butane mixtures).

| $x^*$ ($CH_4$ %) | LFLs** | | | | UFLs** | | | |
|---|---|---|---|---|---|---|---|---|
| | This Research | Le Chatelier's | Dev | Dev % | This Research | Le Chatelier's | Dev | Dev % |
| 0 | 1.72 | 1.72 | 0.00 | 0.00 | 8.46 | 8.46 | 0.00 | 0.00 |
| 12.5 | 1.86 | 1.88 | -0.02 | 0.96 | 8.91 | 8.98 | -0.07 | 0.80 |
| 25 | 2.05 | 2.07 | -0.02 | 0.86 | 9.48 | 9.57 | -0.09 | 0.97 |
| 37.5 | 2.29 | 2.30 | -0.01 | 0.43 | 10.11 | 10.24 | -0.13 | 1.33 |
| 50 | 2.56 | 2.59 | -0.03 | 1.22 | 10.83 | 11.02 | -0.19 | 1.75 |
| 62.5 | 2.95 | 2.97 | -0.02 | 0.57 | 11.82 | 11.92 | -0.10 | 0.86 |
| 75 | 3.49 | 3.47 | 0.02 | 0.58 | 12.71 | 12.98 | -0.27 | 2.15 |
| 87.5 | 4.19 | 4.18 | 0.01 | 0.28 | 14.12 | 14.25 | -0.13 | 0.95 |
| 100 | 5.25 | 5.25 | 0.00 | 0.00 | 15.80 | 15.80 | 0.00 | 0.00 |

* Percentage fractions of methane in methane and n-butane mixtures
** Data obtained at room temperature and atmospheric pressure

**Methane and ethylene mixtures:** Table 4.6 shows the experimental data and their absolute and relative deviations from the predictions of Le Chatelier's Law for the lower and upper flammability limits of methane and ethylene mixtures. In the case of lower flammability limits estimation, Le Chatelier's formula can be used without modification (Eq. (28)); while for upper flammability limits estimation, modification of Le Chatelier's Law was conducted as Eq. (29), and the best fitting curve to the experimental data was presented in Figure 4.19.

$$\frac{1}{LFL_{methana/ethylene}} = \frac{x}{LFL_{methane}} + \frac{(1-x)}{LFL_{ethylene}} \tag{28}$$

$$\frac{1}{UFL_{methana/ethylene}} = \frac{x^{1.3}}{UFL_{methane}} + \frac{(1-x)^{0.6}}{UFL_{ethylene}} \tag{29}$$

Table 4.6 Flammability limit data from experimental measurements and Le Chatelier's Law (methane and ethylene mixtures).

| $x^*$ ($CH_4$ %) | LFLs** | | | | UFLs** | | | |
|---|---|---|---|---|---|---|---|---|
| | This Research | Le Chatelier's | Dev | Dev % | This Research | Le Chatelier's | Dev | Dev % |
| 0 | 2.81 | 2.81 | 0.00 | 0.00 | 30.61 | 30.61 | 0.00 | 0.00 |
| 12.5 | 3.01 | 2.98 | 0.03 | 0.89 | 29.62 | 27.40 | 2.22 | 7.50 |
| 25 | 3.20 | 3.18 | 0.02 | 0.64 | 26.66 | 24.80 | 1.86 | 6.98 |
| 37.5 | 3.37 | 3.40 | -0.03 | 0.98 | 23.54 | 22.65 | 0.89 | 3.79 |
| 50 | 3.68 | 3.66 | 0.02 | 0.53 | 20.59 | 20.84 | -0.25 | 1.22 |
| 62.5 | 4.01 | 3.96 | 0.05 | 1.24 | 18.34 | 19.30 | -0.96 | 5.25 |
| 75 | 4.30 | 4.31 | -0.01 | 0.32 | 17.11 | 17.97 | -0.86 | 5.05 |
| 87.5 | 4.71 | 4.74 | -0.03 | 0.55 | 16.55 | 16.82 | -0.27 | 1.61 |
| 100 | 5.25 | 5.25 | 0.00 | 0.00 | 15.80 | 15.80 | 0.00 | 0.00 |

* Percentage fractions of methane in methane and ethylene mixtures
** Data obtained at room temperature and atmospheric pressure

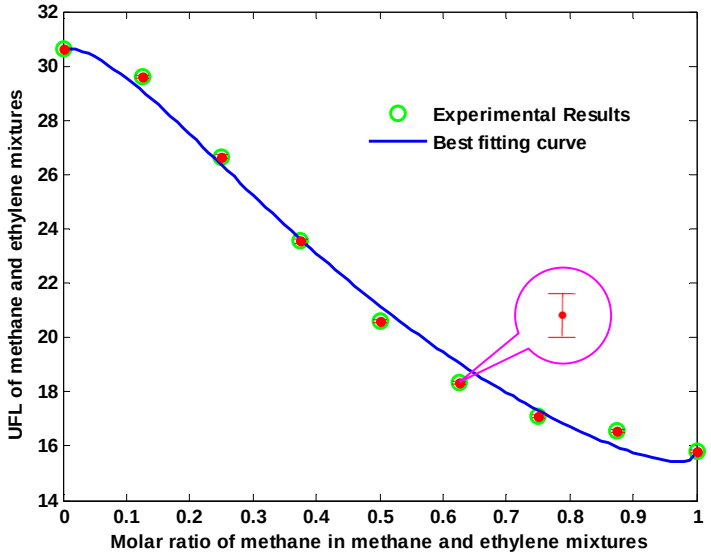


Fig. 4.19. Best fitting curve for UFLs of methane and ethylene mixtures at standard conditions.

**Methane and acetylene:** Table 4.7 shows the experimental data and their absolute and relative deviations from the predictions of Le Chatelier's Law for the lower and upper flammability limits of methane and acetylene mixtures. Le Chatelier's Law can be directly used to estimate the LFLs of the mixtures without modification (Eq. (30)). For upper flammability limits estimation, modification of Le Chatelier's Law was used as shown in Eq. (31), and the best fitting curve to the experimental data is presented in Figure 4.20.

$$\frac{1}{LFL_{methana/acetylene}} = \frac{x}{LFL_{methane}} + \frac{(1-x)}{LFL_{acetylene}} \tag{30}$$

$$\frac{1}{UFL_{methana/acetylene}} = \frac{x^{2.1}}{UFL_{methane}} + \frac{(1-x)^{0.3}}{UFL_{acetylene}} \tag{31}$$

Table 4.7 Flammability limit data from experimental measurements and Le Chatelier's Law (methane and acetylene mixtures).

| $x^*$ ($CH_4$ %) | **LFLs**** | | | | **UFLs**** | | | |
|---|---|---|---|---|---|---|---|---|
| | This Research | Le Chatelier's | Dev | Dev % | This Research | Le Chatelier's | Dev | Dev % |
| 0 | 2.42 | 2.42 | 0.00 | 0.00 | 77.31 | 77.31 | 0.00 | 0.00 |
| 12.5 | 2.61 | 2.59 | 0.02 | 0.58 | 72.12 | 52.00 | 20.12 | 27.89 |
| 25 | 2.83 | 2.80 | 0.03 | 1.17 | 60.53 | 39.18 | 21.35 | 35.27 |
| 37.5 | 3.00 | 3.03 | -0.03 | 1.10 | 51.24 | 31.43 | 19.81 | 38.66 |
| 50 | 3.26 | 3.31 | -0.05 | 1.62 | 46.07 | 26.24 | 19.83 | 43.05 |
| 62.5 | 3.68 | 3.65 | 0.03 | 0.83 | 31.45 | 22.52 | 8.93 | 28.40 |
| 75 | 4.08 | 4.06 | 0.02 | 0.43 | 22.38 | 19.72 | 2.66 | 11.87 |
| 87.5 | 4.55 | 4.58 | -0.03 | 0.67 | 19.46 | 17.54 | 1.92 | 9.84 |
| 100 | 5.25 | 5.25 | 0.00 | 0.00 | 15.80 | 15.80 | 0.00 | 0.00 |

* Percentage fractions of methane in methane and acetylene mixtures
** Data obtained at room temperature and atmospheric pressure

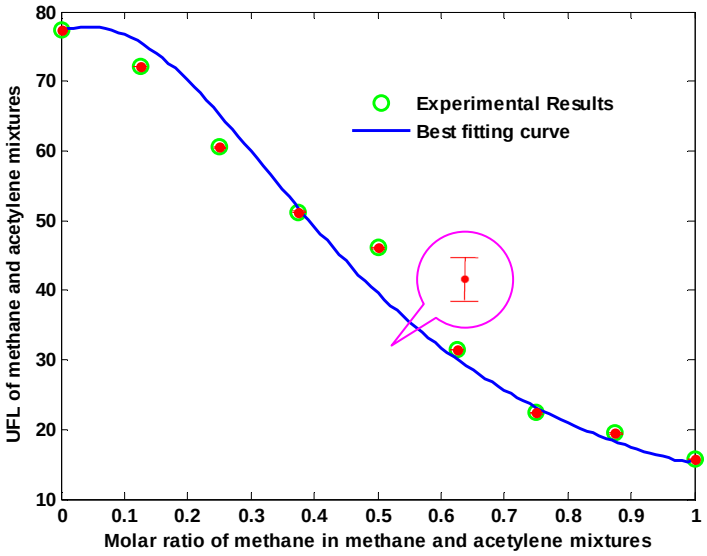


Fig. 4.20. Best fitting curve for UFLs of methane and acetylene mixtures at standard conditions.

**Ethylene and propylene:** Table 4.8 shows the experimental data and their absolute and relative deviations from the predictions of Le Chatelier's Law for the lower and upper flammability limits of ethylene and propylene mixtures. Based on information shown in the table, Le Chatelier's Law can be directly used to estimate the LFLs of the mixtures (Eq. (32)). For upper flammability limits estimation, modification of Le Chatelier's Law was used as shown in Eq. (33), and the best fitting curve to the experimental data is presented in Figure 4.21.

$$\frac{1}{LFL_{ethylene\,/\,propylene}} = \frac{x}{LFL_{ethylene}} + \frac{(1-x)}{LFL_{propylene}} \tag{32}$$

$$\frac{1}{UFL_{ethylene\,/\,propylene}} = \frac{x^{0.3}}{UFL_{ethylene}} + \frac{(1-x)^{1.3}}{UFL_{propylene}} \tag{33}$$

Table 4.8 Flammability limit data from experimental measurements and Le Chatelier's Law (ethylene and propylene mixtures).

| $x^*$ ($C_2H_4$ %) | LFLs** | | | | UFLs** | | | |
|---|---|---|---|---|---|---|---|---|
| | This Research | Le Chatelier's | Dev | Dev % | This Research | Le Chatelier's | Dev | Dev % |
| 0 | 2.28 | 2.28 | 0.00 | 0.00 | 10.25 | 10.25 | 0.00 | 0.00 |
| 12.5 | 2.32 | 2.34 | -0.02 | 0.65 | 10.38 | 11.18 | -0.80 | 7.70 |
| 25 | 2.43 | 2.39 | 0.04 | 1.53 | 11.66 | 12.29 | -0.63 | 5.44 |
| 37.5 | 2.41 | 2.45 | -0.04 | 1.81 | 12.81 | 13.66 | -0.85 | 6.61 |
| 50 | 2.52 | 2.52 | 0.00 | 0.10 | 14.04 | 15.36 | -1.32 | 9.38 |
| 62.5 | 2.55 | 2.58 | -0.03 | 1.36 | 17.31 | 17.54 | -0.23 | 1.34 |
| 75 | 2.64 | 2.66 | -0.02 | 0.59 | 22.64 | 20.45 | 2.19 | 9.66 |
| 87.5 | 2.75 | 2.73 | 0.02 | 0.70 | 27.23 | 24.52 | 2.71 | 9.95 |
| 100 | 2.81 | 2.81 | 0.00 | 0.00 | 30.61 | 30.61 | 0.00 | 0.00 |

* Percentage fractions of ethylene in ethylene and propylene mixtures
** Data obtained at room temperature and atmospheric pressure

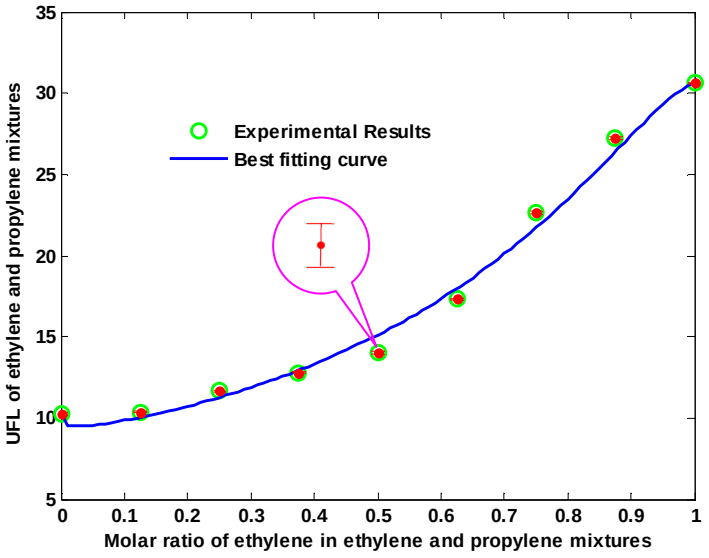


Fig. 4.21. Best fitting curve for UFLs of ethylene and propylene mixtures at standard conditions.

**Ethylene and acetylene:** Table 4.9 shows the experimental data and their absolute and relative deviations from the predictions of Le Chatelier's Law for the lower and upper flammability limits of ethylene and acetylene mixtures. In the case of lower flammability limits estimation, Le Chatelier's formula can be used without modification (Eq. (34)); while for upper flammability limits estimation, modification of Le Chatelier's Law was used as shown in Eq. (35), and the best fitting curve to the experimental data is presented in Figure 4.22.

$$\frac{1}{LFL_{ethylene/acetylene}} = \frac{x}{LFL_{ethylene}} + \frac{(1-x)}{LFL_{acetylene}} \tag{34}$$

$$\frac{1}{UFL_{ethylene/acetylene}} = \frac{x}{UFL_{ethylene}} + \frac{(1-x)^{1.3}}{UFL_{acetylene}} \tag{35}$$

Table 4.9 Flammability limit data from experimental measurements and Le Chatelier's Law (ethylene and acetylene mixtures).

| $x^*$ ($C_2H_4$ %) | **LFLs**** | | | | **UFLs**** | | | |
|---|---|---|---|---|---|---|---|---|
| | This Research | Le Chatelier's | Dev | Dev % | This Research | Le Chatelier's | Dev | Dev % |
| 0 | 2.42 | 2.42 | 0.00 | 0.00 | 77.31 | 77.31 | 0.00 | 0.00 |
| 12.5 | 2.44 | 2.46 | -0.02 | 0.93 | 67.42 | 64.93 | 2.49 | 3.70 |
| 25 | 2.50 | 2.51 | -0.01 | 0.28 | 58.21 | 55.96 | 2.25 | 3.86 |
| 37.5 | 2.58 | 2.55 | 0.03 | 1.05 | 52.36 | 49.18 | 3.18 | 6.08 |
| 50 | 2.61 | 2.60 | 0.01 | 0.37 | 45.54 | 43.86 | 1.68 | 3.70 |
| 62.5 | 2.68 | 2.65 | 0.03 | 1.12 | 42.12 | 39.57 | 2.55 | 6.04 |
| 75 | 2.68 | 2.70 | -0.02 | 0.79 | 38.66 | 36.05 | 2.61 | 6.74 |
| 87.5 | 2.72 | 2.75 | -0.03 | 1.27 | 35.25 | 33.11 | 2.14 | 6.07 |
| 100 | 2.81 | 2.81 | 0.00 | 0.00 | 30.61 | 30.61 | 0.00 | 0.00 |

* Percentage fractions of ethylene in ethylene and acetylene mixtures
** Data obtained at room temperature and atmospheric pressure

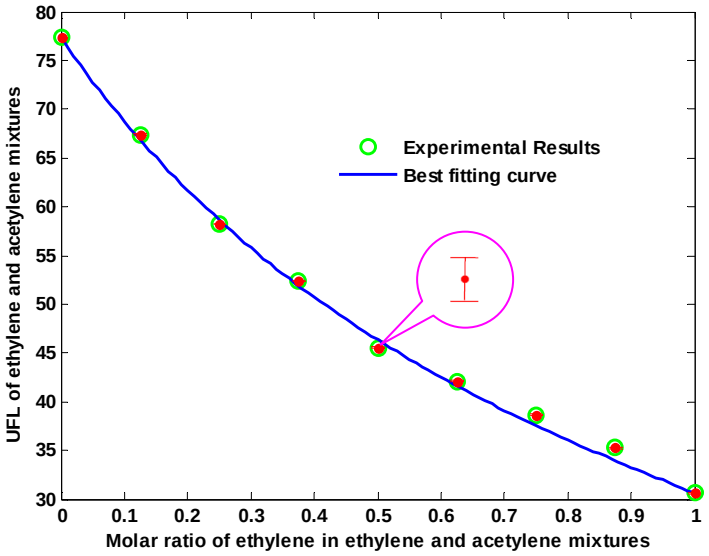


Fig. 4.22. Best fitting curve for UFLs of ethylene and acetylene mixtures at standard conditions.

4.5.2 Correlations between Stoichiometric Concentrations and Flammability Limits for Binary Hydrocarbon Mixtures

Fuel stoichiometric concentration is the fuel content by which all the reactants could be completely and exactly consumed by the combustion reaction. To corelate the stoichiometric concentrations with flammability limits for the above fuel mixtures, the ratios (stoichiomethric concentrations to lower flammability limits, and stoichiomethric concentrations to upper flammability limits) were quantitatively characterized with fuel molar fractions. Table 4.10 shows the results expressed as a linear function for the subcategory of lower flammability limits, and a quadratic function for the upper flammability limits, in which different fuel combinations have different coefficients except methane and n-butane mixtures ($LFL/C_{st}$ equals 0.55).

Table 4.10. Correlations between the flammability limits and the stoichiometric concentrations for binary hydrocarbon mixtures.

| Fuel1/Fuel2 mixtures | $LFL_{mix}/C_{st\text{-}mix}$* | | $UFL_{mix}/C_{st\text{-}mix}$** | | |
|---|---|---|---|---|---|
| | $a_L$ | $b_L$ | $a_U$ | $b_U$ | $c_U$ |
| $CH_4$/n-$C_4H_{10}$ | $LFL_{mix}/C_{st\text{-}mix}$ = 0.55 | | 2.030 | -5.249 | 4.837 |
| $CH_4/C_2H_4$ | 0.118 | 0.423 | -0.497 | -0.521 | 2.695 |
| $CH_4/C_2H_2$ | 0.242 | 0.283 | 3.550 | -12.468 | 10.304 |
| $C_2H_4/C_3H_6$ | -0.082 | 0.514 | 2.974 | -0.366 | 2.266 |
| $C_2H_4/C_2H_2$ | 0.116 | 0.311 | 3.267 | -8.283 | 9.894 |

* $$\frac{LFL_{mix}}{C_{st,mix}} = a_L \cdot x_{Fuel1} + b_L$$

** $$\frac{UFL_{mix}}{C_{st,mix}} = a_U \cdot x_{Fuel1}^{\ 2} + b_U \cdot x_{Fuel1} + c_U$$

$x_{fuel1}$ Molar fractions (0 ~ 1) of fuel1 in fuel1 and fuel2 mixtures

## 4.6 Conclusions

In this research, the flammability limits of binary hydrocarbon mixtures at standard conditions (room temperature and atmospheric pressure) were estimated employing an innovative detection criterion, in which five thermistors worked as the flame propagation detector, and one dynamic transducer was used to record pressure change to confirm the occurrence of combustion. Through experimental calibration, flammability limits were estimated from the probabilities of temperately continuous flame propagation with different fuel concentrations.

Five hydrocarbons were selected as the experimental samples in this research, which include two saturated components (methane and n-butane), two double-bonded components (ethylene and propylene) and one triple-bonded component (acetylene). The lower flammability limits and upper flammability limits of the fuel mixtures from these

hydrocarbons were measured. The binary hydrocarbon combinations consisted of methane and n-butane, methane and ethylene, methane and acetylene, ethylene and propylene, and ethylene and acetylene.

By comparing experimental data with Le Chatelier's Law, we found that the lower flammability limits of binary hydrocarbon mixtures can be fit by Le Chatelier's Law very well; for upper flammability limits of fuel mixtures which contain two saturated hydrocarbons, the experimental observations can be roughly fit by Le Chatelier's Law; however, for upper flammability limits of fuel mixtures containing one unsaturated components at least, modification of Le Chatelier's Law is needed based on the experimental data.

Le Chatelier's law was modified by powering the percentage concentrations of fuels from maximum R-square values. For different fuel combinations, the powering values were different and there seems no direct connection among them. Moreover, the experimentally measured flammability limits were related to the stoichiometric concentrations, in which the linear function was preferred for the lower flammability limit quantifications. The quadratic function expression for the upper flammability limit conditions fit these data much better than a linear function.

# CHAPTER V

# CFT-V MODELING TO ESTIMATE THE LOWER FLAMMABILITY LIMITS OF BINARY HYDROCARBON MIXTURES

## 5.1 Overview

CFT-V is the abbreviation of Calculated Flame Temperature at constant Volume. Previous research defined two adiabatic flame temperatures: one for constant-pressure combustion and one for constant-volume combustion. These two temperatures would be reached if a fuel-air mixture could react without heat loss to the environment. In this research, CFT-V modeling is the extended application of Calculated Adiabatic Flame Temperature (CAFT) modeling to estimate the flammability limits of fuels. The guiding equation to develop this modeling is heat balance, which is a comprehensive consideration of energy conservation, put differently, the system internal energy change equals the heat exchanges in three basic mechanisms of heat transfer (heat conduction, heat convection, and heat radiation) and work exerted on the system. Because heat transfer is a geometrically-related phenomenon, the reaction vessel configuration affects the calculated flame temperature at constant volume, and accordingly, the predicted flammability limits using this model is a function of the reactor configuration.

In this research, CFT-V modeling was used to estimate the lower flammability limits because of the theoretical availability to calculate the flame temperature at the lower flammability limit condition, in which all the fuel is exhausted completely during the interval of flame propagation. The final products of combustion can be

conservatively estimated to be carbon dioxide, steam vapor and the remaining air. Meanwhile, homogeneous mixing is assumed during the process of fuel/air mixture burning. Thermal energy losses to the environment include two mechanisms: (i) Natural convection away from the reaction vessel outside surface; and (ii) Absorption into the reaction vessel wall. Based on experimental observations, the measured fuel/air flame propagation interval is very short (~1 sec). For easily handled calculations, heat transfer will be assumed to happen at the outside surface of the reaction vessel only.

CFT-V modeling predictions are compared with experimental observations for modeling effectiveness evaluation. The effect of heat losses on flammability limits are evaluated as well by using this modeling with/without the consideration of heat losses. Because flammability limits are highly related to the final flame temperature in the CFT-V modeling application, lower flammability limits predictions using different flame temperature methods are conducted as well. Finally, CAFT modeling is applied in this research, by which the estimations are compared with predictions using CFT-V modeling.

Because CFT-V modeling is based on a comprehensive energy conservation analysis, in which the energy loss is related to the fuel combustion chamber setup, its application is limited. If the heat loss is negligible, CFT-V modeling is similar to CAFT modeling except the heat capacity (at constant volume for CFT-V; at constant pressure for CAFT) and combustion energy quantification ($\Delta E$ for CFT-V; $\Delta H$ for CAFT).

## 5.2 CFT-V Model Construction

The first law of thermodynamics was applied as a general equation for the CFT-V modeling development (Eq. (36)), where the internal energy change ($\Delta U$) of the analyzed system equals the absolute internal energy difference between the final ($U_f$) and initial ($U_i$) conditions, or the internal energy change is triggered by the external "driving forces", for example, the work ($W$) acting on the system and heat exchange ($Q$) between the system and the external environment.

$$\Delta U = U_f - U_i = W + Q \tag{36}$$

This CFT-V modeling applies to a constant-volume system with a comprehensive consideration of energy balance based on the experimental apparatus of this research. The work ($W$) in Eq. (36) can be set to zero because there is no volume work (constant volume) and no shaft work input. Heat exchange ($Q$) is only related to heat losses from the reaction vessel, which is dependent on the apparatus configuration. Internal energy change ($\Delta U$) can be subdivided into two parts: an internal energy change ($\Delta U_1$) from the fuel/air mixture combustion at initial temperature expressed as Eq. (37), and an internal energy change ($\Delta U_2$) using combustion energy to heat reaction products from initial temperature ($T_0$) to the final flame temperature ($T_F$), which is illustrated in Eq. (38). Because the internal energy is a state function, the summation of these two subdivisions must equal the total internal energy change. Then by combining Eq. (36), Eq. (37), and Eq. (38), we obtain the final governing equation expression as Eq. (39).

$$\Delta U_1 = -\Delta E_c = -\left(\Delta H_c + \Delta nRT_0\right) \tag{37}$$

$$\Delta U_2 = \sum_{prods} n_j \int_{T_0}^{T_F} C_{Vi} dT = f(T_F) \tag{38}$$

$$Q + (\Delta H_c + \Delta nRT_0) = \sum_{prods} n_j \int_{T_0}^{T_F} C_{Vi} dT \tag{39}$$

where $\Delta E_c$ is the energy of combustion at the initial temperature; $\Delta H_c$ is the enthalpy of combustion at initial temperature, which is the negative to the enthalpy change in the chemical reaction; $R$ is universal gas constant; $\Delta n$ = (gaseous moles of products – gaseous moles of reactants); $n_j$ is total mole number of product $j$; $C_{Vi}$ is the constant-volume heat capacity, which is a function of temperature.

**5.3 Prediction Methodology Using CFT-V Modeling**

The purpose of CFT-V modeling is to estimate lower flammability limits of binary hydrocarbon mixtures. The application of CFT-V modeling is a four-step procedure (shown in Figure 5.1): (i) Collection of the lower flammability data for pure hydrocarbons; (ii) Calculation of the final flame temperatures for every pure hydrocarbon at the concentration of lower flammability limits; (iii) Estimation of the final flame temperature of hydrocarbon mixtures using data obtained in (ii); and (iv) Determination of the flammability limits of hydrocarbon mixtures.

5.3.1 Flammability Limits of Pure Hydrocarbons

Flammability data for pure hydrocarbons (methane, n-butane, ethylene, propylene, and acetylene) were collected from experimental measurements developed in this research (Table 5.1). Based on previous research, the flammability limits are dependent on the experimental setup and the flammability data vary with experimental apparatus and detection criteria. CFT-V modeling is the application of heat balance,

which is sensitive to the experimental configuration. Therefore, keeping these data sources consistent with CFT-V modeling situation is preferred for higher accuracy.

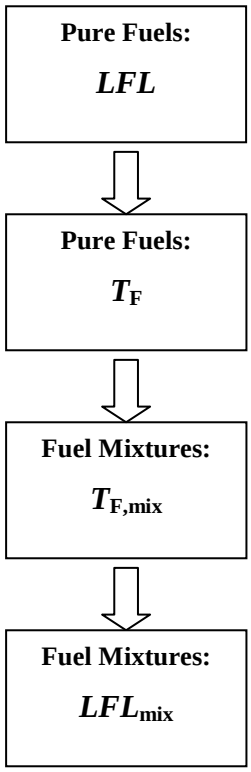


Fig. 5.1. Procedure to estimate LFLs of binary hydrocarbon mixtures using CFT-V modeling.

Table 5.1. Experimentally measured flammability data from this research.

| Fuels | LFL (%) | UFL (%) |
|---|---|---|
| $CH_4$ | 5.25 | 15.80 |
| n- $C_4H_{10}$ | 1.72 | 8.46 |
| $C_2H_4$ | 2.81 | 30.61 |
| $C_3H_6$ | 2.28 | 10.25 |
| $C_2H_2$ | 2.42 | 77.31 |

5.3.2 Estimating Flame Temperatures of Pure Hydrocarbons.

From the CFT-V modeling governing equation, Eq. (39), the final flame temperature ($T_F$) can be calculated as one variable by estimating the values of heat exchange ($Q$), energy of combustion at the initial temperature ($\Delta H_c+\Delta nRT_0$), and the mole numbers of product $n_j$ in advance.

**Energy of Combustion:** At the initial temperature ($T_0$ = 25 ºC), the enthalpy of combustion $\Delta H_c$ can be easily calculated from the enthalpy of formation, which is available from the literature as well. $\Delta n$, the total mole number change in a certain reaction, is a function of fuel concentration and fuel constitution. For a general hydrocarbon formula, $C_aH_b$, the total mole change at the fuel concentration of lower flammability limit is obtained based on the complete chemical reaction expression (Eq. (40)). $R$ is a constant. $T_0$ is the initial temperature and set to 25 ºC. Table 5.2 shows the energy of combustions for the selected pure hydrocarbons (methane, n-butane, ethylene, propylene, and acetylene).

$$C_aH_b + \frac{(1-LFL)}{4.77\times LFL}(O_2 + 3.77N_2) \rightarrow$$
$$aCO_2 + \frac{b}{2}H_2O + \frac{3.77\times(1-LFL)}{4.77\times LFL}N_2 + (\frac{1-LFL}{4.77\times LFL} - a - \frac{b}{4})O_2 \quad (40)$$

Table 5.2. Estimation of energy of combustions for pure hydrocarbons.

| **Fuels** | $\Delta H_c$ (kJ/mol-fuel) | $\Delta n$ (mol/mol-fuel) | $\Delta nRT$ (kJ/mol-fuel) | $\Delta E_c$ (kJ/mol-fuel) |
|---|---|---|---|---|
| $CH_4$ | 802.3 | 0 | 0 | 802.3 |
| n- $C_4H_{10}$ | 2656.0 | 1.5 | 3.72 | 2659.7 |
| $C_2H_4$ | 1323.1 | 0 | 0 | 1323.1 |
| $C_3H_6$ | 1926.4 | 0.5 | 1.24 | 1927.6 |
| $C_2H_2$ | 1255.5 | -0.5 | -1.24 | 1254.3 |

**Energy exchange between the reaction vessel and the environment:** Based on this research's experimental setup, the energy exchange between the reaction vessel and environment only results from the heat losses. The reaction vessel is a cylindrical combustion chamber (schedule 40, 4 inch nominal and 316 SS stainless steel) with I.D. 10.22 cm, O.D. 11.43 cm, length 100 cm, and total volume 8.2 liter. Heat loss starts from both convective and radiative heat transfer from the fuel gases and flame, respectively, to the inside surface of the reaction vessel, then followed by heat conduction through the vessel wall, and eventually transferred away by natural convection on the outside of the vessel (Figure 5.2). Specifically, in this case, energy loss includes natural heat convection to the external environment and heat absorption by the reaction vessel wall during the process of fuel/air mixture ignition, flame propagation, and flame exhaustion, Heat radiation into ambient air is negligible because of an extremely minor temperature change at the outside surface of the reaction vessel, and heat conduction into air can also be ignored compared to the heat convection.

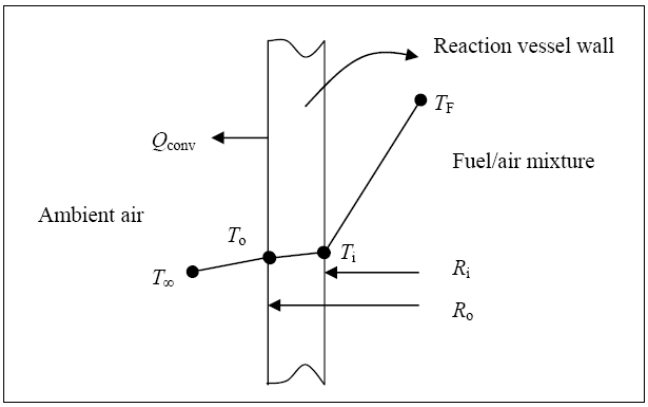


Fig 5.2. Cross section of reaction vessel wall with heat transfers and temperature distributions.

The total heat loss $Q_{total}^{s}$ from the reaction system can be calculated using Eq. (41), which indicates that heat convection $Q_{conv,i}$ from the inside surface of the reaction vessel equals the summation of heat absorption $Q_{abs}$ into reaction vessel wall and heat natural convection $Q_{conv,o}$ to ambient air through the outside surface of the reaction vessel.

$$Q_{total}^{s} = Q_{conv,i} = Q_{abs} + Q_{conv,o} \tag{41}$$

Theoretically, the total heat convection (Eq. (42)) from the reaction system into the reaction vessel can be calculated using Fourier's heat flow rate equation (Eq. (43)).

$$Q_{conv,i} = \alpha q_{conv,i} \Delta t \tag{42}$$

$$q_{conv,i} = \frac{(T_F - T_i)}{\frac{1}{h_i 2\pi R_i L}} = \frac{(T_F - T_\infty)}{\frac{1}{h_i 2\pi R_i L} + \frac{\ln(R_o / R_i)}{2\pi k L} + \frac{1}{h_o 2\pi R_o L}} \tag{43}$$

where, $q_{\mathrm{conv,i}}$ is the heat flow rate from the reaction system to the inside surface of the reaction vessel. $\alpha$ is the heat loss effectiveness factor, 0.5 was assumed based on an imaginary situation, in which the temperature between the ignition source to the flame front is constant (equal to the flame temperature) and the temperature from flame front to the top of the reaction vessel is the initial temperature of the fuel/air mixture. $\Delta t$ is the flame travel duration from the fuel/air mixture ignition to flame exhaustion. The flame travel time from ignition source to the top of the reaction vessel is about 1.1 sec in the case of the temperately continuous flame propagation (based on the experimental temperature profiles recorded by five themistors). $T_{\mathrm{F}}$ is the flame temperature, which

would change with the combustion fuel. $T_\infty$ is the ambient air temperature, 25 ºC in this case. $T_i$, $T_o$ are the temperatures of the reactor inside and outside surfaces. $L$ is the distance from the ignition source to the quenching point (85 cm was taken, because the interval from the fuse igniter to the farthest thermistor is 75 cm, and plus the average distance 10 cm in which the flame may propagate continuously beyond the farthest thermistor or the flame may propagate downward). $R_i$ and $R_o$ are inside and outside radiuses of the reaction vessel, respectively. $h_i$, $h_o$ are convective heat transfer coefficients at the inside and outside surfaces of the reaction vessel. $k$ is the thermal conductivity of the reaction vessel wall.

Heat flow equation (Eq. (43) can be simplified to Eq. (44). Because convective heat transfer coefficient is not a material constant and it dramatically depends on temperature difference in the region where the heat convection occurs, the value of $h_o$ would be much higher than $h_i$ (approximate 5 W/m$^2$K from John Zink Combustion Handbook [48]), and the thermal resistance at the outside surface of the reaction vessel can be ignored compared with the one at the inside surface of the vessel. Based on temperature measurement information (temperature profiles are approximately illustrated in 5.2), $T_o$ is very close to $T_\infty$, and $T_i$ is close to $T_o$ as well due to the high conductivity of reaction vessel wall (13.57 W/m-K[49] for 316 SS stainless steel), while $T_F$ sharply drops to $T_i$ .

$$q_{conv,i} = \frac{(T_F - T_\infty)}{\frac{1}{h_i 2\pi R_i L} + \frac{\ln(R_o / R_i)}{2\pi k L} + \frac{1}{h_o 2\pi R_o L}} = \frac{(T_F - T_\infty)}{\frac{1}{h_i 2\pi R_i L} + \frac{\ln(R_o / R_i)}{2\pi k L}} \tag{44}$$

Now, converting the total heat loss in the reaction vessel to the total heat loss $Q$ for one mole of fuel, we can obtain Eq. (45), where $Q$ is a function of the flame temperature for different pure hydrocarbons (methane, n-butane, ethylene, propylene, and acetylene).

$$Q = \frac{Q_{total}^{s} RT_0}{LFL \times P_0 V_R} \tag{45}$$

where, LFL is the lower flammability limit for a certain pure hydrocarbon. $T_0$ is the initial temperature of fuel/air mixture (25 ºC). $V_R$ is the reaction vessel chamber volume (8.2 liter). $P_0$ is the initial pressure (1 atm) of the fuel/air mixture.

**Mole numbers of products**: The mole numbers of product $n_j$ can be computed using the chemical reaction equation (Eq. (40)). Table 5.3 shows the moles numbers per mole of pure hydrocarbon of reaction products (carbon dioxide, steam vapor, inert gas nitrogen and the remaining oxygen). The heat capacities at constant pressure of these products are listed in Table 5.4. The difference between the heat capacity at constant pressure and at constant volume is the universal gas constant for ideal gases.

Table 5.3. Final product molar numbers per mole of pure hydrocarbons.

| **Fuel** | $\boldsymbol{n_j}$ (mole/mole-fuel) | | | |
|---|---|---|---|---|
| | $\boldsymbol{CO_2}$ (mol/mol-fuel) | $\boldsymbol{H_2O}$ *(g)* (mol/mol-fuel) | $\boldsymbol{N_2}$ (mol/mol-fuel) | $\boldsymbol{O_2}$ (mol/mol-fuel) |
| $CH_4$ | 1 | 2 | 14.26 | 1.78 |
| n- $C_4H_{10}$ | 4 | 5 | 45.16 | 5.48 |
| $C_2H_4$ | 2 | 2 | 27.34 | 4.25 |
| $C_3H_6$ | 3 | 3 | 33.87 | 4.46 |
| $C_2H_2$ | 2 | 1 | 33.47 | 5.95 |

Table 5.4. Heat capacities at constant pressure for reaction products.

| **Products** | $C_p = a + b \cdot T + c \cdot T^2 + d \cdot T^3$ (J/mol•K) | | | |
|---|---|---|---|---|
| | ***a*** | ***b**10$^2$** | ***c**10$^5$** | ***d**10$^9$** |
| ***$CO_2$*** | 22.243 | 5.977 | -3.499 | 7.464 |
| ***$H_2O$ (g)*** | 32.218 | 0.192 | 1.055 | -3.593 |
| ***$N_2$*** | 28.883 | -0.157 | 0.808 | -2.971 |
| ***$O_2$*** | 25.460 | 1.519 | -0.715 | 1.311 |

Now recalling the CFT-V modeling governing equation (Eq. (39)) and inputting the energy of combustion ($\Delta E_c$), heat loss ($Q$), and final mole numbers of products ($n_j$) for different hydrocarbons, we can obtain a function of only one variable, the final flame temperature ($T_F$). Using Matlab® software, the flame temperatures for pure hydrocarbons were obtained (Table 5.5).

Table 5.5. Calculated flame temperature for pure hydrocarbon.

| Fuels | $T_F$ (K) ***CFT-V*** | $T_{ad}$ (K) (**Reference** [50]) |
|---|---|---|
| $CH_4$ | 1768 | 1650 |
| n- $C_4H_{10}$ | 1843 | 1765 |
| $C_2H_4$ | 1626 | 1475 |
| $C_3H_6$ | 1811 | 1610 |
| $C_2H_2$ | 1397 | 1275 |

5.3.3 Estimating the Flame Temperature of Hydrocarbon Mixtures.

Some previous research found that almost all hydrocarbons have roughly equal adiabatic flame temperatures at the concentrations of the lower flammability limits (e.g., 1600K from Shebeko et al. [34]); 1200K from Mashuga [35]). The wide applications of CAFT modeling indicated that for accurate quantification of the lower flammability limit, the adiabatic flame temperature for different fuel families should be characterized separately, e.g., if an average adiabatic flame temperature is taken per family group of

hydrocarbons, a value of 1590.59 K will be obtained for the paraffinic group and 1610.50 K for the unsaturated group [51]. Actually, the adiabatic flame temperature is calculated based on the prerequirements of experimental LFLs and the ideal assumption of no heat loss, so accordingly, different experimental setup and external conditions would affect the adiabatic flame temperature. Until now, the extended research on adiabatic flame temperature of fuel mixtures was scarcely conducted. One proper method to estimate the adiabatic flame temperature of fuel mixtures was proposed by Vidal [51] as a linear expression with molar fractions and adiabatic flame temperatures of pure fuels.

This research delivered a comprehensive practice to estimate the flame temperatures of hydrocarbon mixtures based on energy conservation and reaction vessel configuration, in which the lower flammability data were from the experimental measurement part, and energy balance equation Eq. (39) was employed as the computation guiding equation. Given a binary fuel mixture containing Fuel-1 ($C_aH_b$) and Fuel-2 ($C_mH_n$), for each pure fuel combusting at the concentration of the LFL, the final products and the molar productions can be calculated using Eq. (40). Putting these values into Equation 39, and removing the integration operation by using the average heat capacity, the following expression was obtained for Fuel-1 in Eq. (46) and Fuel-2 in Eq. (47).

$$Q_1 + \Delta E_{c,1} = \left[ \begin{array}{l} a\overline{C}_{V,CO_2} + \frac{b}{2}\overline{C}_{V,H_2O} + \frac{3.77(1-LFL_1)}{4.77LFL_1}\overline{C}_{V,N_2} \\ + \left( \frac{1-LFL_1}{4.77LFL_1} - a - \frac{b}{4} \right)\overline{C}_{V,O_2} \end{array} \right] \left(T_{F,1} - T_0\right) \quad (46)$$

$$Q_2+\Delta E_{c,2}=\left[\begin{array}{l} m\overline{C}_{V,CO_2}+\frac{n}{2}\overline{C}_{V,H_2O}+\frac{3.77\left(1-LFL_2\right)}{4.77LFL_2}\overline{C}_{V,N_2} \\ +\left(\frac{1-LFL_2}{4.77LFL_2}-m-\frac{n}{4}\right)\overline{C}_{V,O_2} \end{array}\right]\left(T_{F,2}-T_0\right) \tag{47}$$

Now simplifying Eq. (46) and Eq. (47) by using thermodynamic properties of heat capacity (average heat capacity of nitrogen almost equals to that of oxygen [51]), the results are reexpressed in Eq. (48) and Eq. (49).

$$Q_1+\Delta E_{c,1}=\left[a\left(\overline{C}_{V,CO_2}-\overline{C}_{V,O_2}\right)+\frac{b}{2}\left(\overline{C}_{V,H_2O}-\frac{1}{2}\overline{C}_{V,O_2}\right)+\frac{\left(1-LFL_1\right)}{LFL_1}\overline{C}_{V,N_2}\right]\left(T_{F,1}-T_0\right) \tag{48}$$

$$Q_2+\Delta E_{c,2}=\left[m\left(\overline{C}_{V,CO_2}-\overline{C}_{V,O_2}\right)+\frac{n}{2}\left(\overline{C}_{V,H_2O}-\frac{1}{2}\overline{C}_{V,O_2}\right)+\frac{\left(1-LFL_2\right)}{LFL_2}\overline{C}_{V,N_2}\right]\left(T_{F,2}-T_0\right) \tag{49}$$

Eq. (48) and Eq. (49) can be simplified by eliminating the first two terms in square brackets, because the summation of first two terms averages about 7% of the sum of terms in the square bracket. Eq. (50), Eq. (51) show the results expressed as the inverse of the lower flammability limits.

$$\frac{1}{LFL_1}=\frac{Q_1+\Delta E_{c,1}}{\left(T_{F,1}-T_0\right)\overline{C}_{V,N_2}}+1 \tag{50}$$

$$\frac{1}{LFL_2}=\frac{Q_2+\Delta E_{c,2}}{\left(T_{F,2}-T_0\right)\overline{C}_{V,N_2}}+1 \tag{51}$$

For the binary hydrocarbon mixture of Fuel-1 ($C_aH_b$) with molar fraction $x$ and Fuel-2 ($C_mH_n$) with molar fraction (1-$x$), reusing Eq. (39) and Eq. (40) again, we can

obtain Eq. (52) solving for the inverse of the lower flammability limit of the fuel mixtures.

$$\frac{1}{LFL_{mix}} = \frac{Q_{mix} + \Delta E_{c,mix}}{\left(T_{F,mix} - T_0\right)\overline{C}_{V,N_2}} + 1 \tag{52}$$

Now combining Eq. (50), Eq. (51) and Eq. (52) by applying Le Chatelier' formula, with Eq. (50) multiplied by *x* and Eq. (51) by (1-*x*)), we can get the final result to solve $T_{\mathrm{F,mix}}$ as Eq. (53).

$$\frac{Q_{mix} + \Delta E_{c,mix}}{\left(T_{F,mix} - T_0\right)} = \frac{x\left(Q_1 + \Delta E_{c,1}\right)}{\left(T_{F,1} - T_0\right)} + \frac{\left(1-x\right)\left(Q_2 + \Delta E_{c,2}\right)}{\left(T_{F,2} - T_0\right)} \tag{53}$$

Where, $\Delta E_{\mathrm{c,mix}}$ is the energy of combustion, which can be expressed as Eq. (54). Especially, when heat loss from reaction vessel is negligible, Eq. (53) can be easily simplified to Eq. (55). If the heat loss is not zero but not important compared with the energy of combustion, Eq. (53) can be simplified also as Eq. (55).

$$\Delta E_{c,mix} = x \cdot \Delta E_{c,1} + (1-x) \cdot \Delta E_{c,2} \tag{54}$$

$$\frac{\Delta E_{c,mix}}{\left(T_{F,mix} - T_0\right)} = \frac{x\Delta E_{c,1}}{\left(T_{F,1} - T_0\right)} + \frac{\left(1-x\right)\Delta E_{c,2}}{\left(T_{F,2} - T_0\right)} \tag{55}$$

Applying the same operation procedures to CAFT modeling, the adiabatic flame temperature for fuel mixtures can be solved using Eq. (56).

$$\frac{\Delta H_{c,mix}}{\left(T_{F,mix} - T_0\right)} = \frac{x\Delta H_{c,1}}{\left(T_{F,1} - T_0\right)} + \frac{\left(1-x\right)\Delta H_{c,2}}{\left(T_{F,2} - T_0\right)} \tag{56}$$

where $\Delta H_{\mathrm{c,mix}}$ is the enthalpy of combustion, which can be expressed as Eq. (57).

$$\Delta H_{c,mix} = x \cdot \Delta H_{c,1} + (1-x) \cdot \Delta H_{c,2} \tag{57}$$

5.3.4 Estimation of the Lower Flammability Limits for Binary Hydrocarbon Mixtures.

Again, the governing equation (Eq. (39)) was used to calculate the lower flammability limits of binary hydrocarbon mixtures. In the equation, heat loss is estimated using Eq. (45), where the $LFL_{\mathrm{mix}}$ can be substituted for *LFL*, determinations of $Q_{total}^{s}$ for fuel mixtures are conducted using the same ways as the pure hydrocarbons. The energy of combustion ($\Delta E_{\mathrm{c,mix}}$) can be solved through Eq. (54) at different fuel molar fractions. The molar production of each product was obtained by applying the chemical reaction equation (Eq. 58), and the results are presented in Table 5.6.

$$LFL_{mix}\left[xC_aH_b+(1-x)C_mH_n\right]+\frac{(1-LFL_{mix})}{4.77}(O_2+3.77N_2)\rightarrow$$
$$\left[aLFL_{mix}x+mLFL_{mix}(1-x)\right]CO_2+\frac{bLFL_{mix}x+nLFL_{mix}(1-x)}{2}H_2O+\frac{3.77\times(1-LFL_{mix})}{4.77}N_2$$
$$+\left\{\frac{1-LFL_{mix}}{4.77}-\left[aLFL_{mix}x+mLFL_{mix}(1-x)\right]-\frac{bLFL_{mix}x+nLFL_{mix}(1-x)}{4}\right\}O_2 \qquad (58)$$

Table 5.6. Products' molar numbers per mole of binary hydrocarbons mixtures.

| Fuels | Product ($n_j$) | | | |
|---|---|---|---|---|
| | $CO_2$ (mol/mol-fuel) | $H_2O$ (g) (mol/mol-fuel) | $N_2$ (mol/mol-fuel) | $O_2$ (mol/mol-fuel) |
| Mixtures ($C_aH_b/C_mH_n$) | $x\cdot a+(1-x)\cdot m$ | $\frac{1}{2}x\cdot b+\frac{1}{2}(1-x)\cdot n$ | $\frac{3.77\cdot(1-LFL_{mix})}{4.77\cdot LFL_{mix}}$ | $\frac{1-LFL_{mix}}{4.77LFL_{mix}}-[x\cdot a+(1-x)\cdot m]-\frac{x\cdot b+(1-x)\cdot n}{4}$ |

Based on the above calculations using CFT-V modeling, the final results are illustrated in Figure 5.3 - 5.7 for the binary hydrocarbon mixtures of methane and n-butane, methane and ethylene, methane and acetylene, ethylene and propylene, ethylene

and acetylene, respectively. The information presented in all these figures indicates that the CFT-V model can fit the experimental observations well.

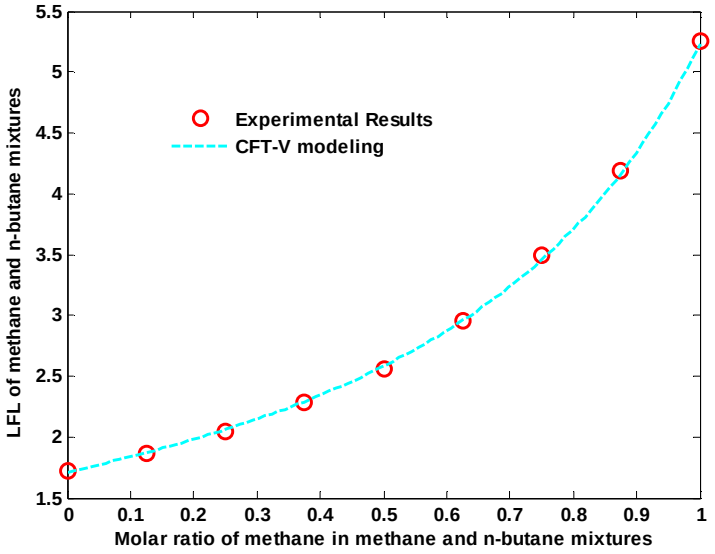


Fig. 5.3. Estimation of LFLs of methane and n-butane mixtures using CFT-V modeling at standard conditions.

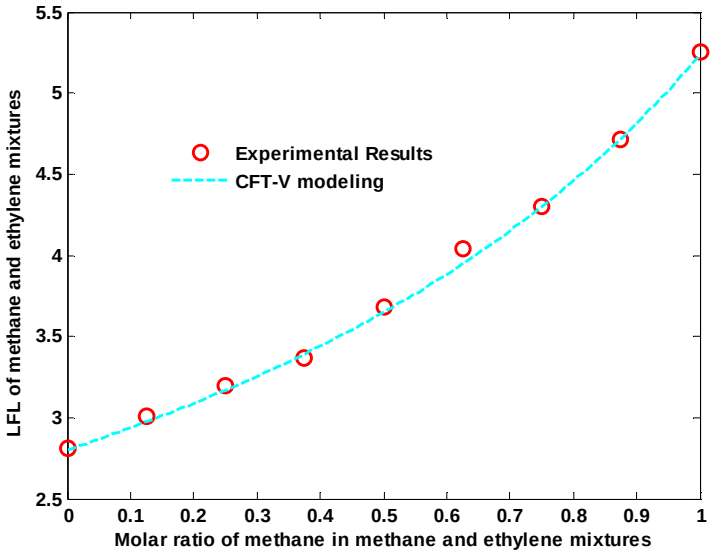


Fig. 5.4. Estimations of LFLs of methane and ethylene mixtures using CFT-V modeling at standard conditions.

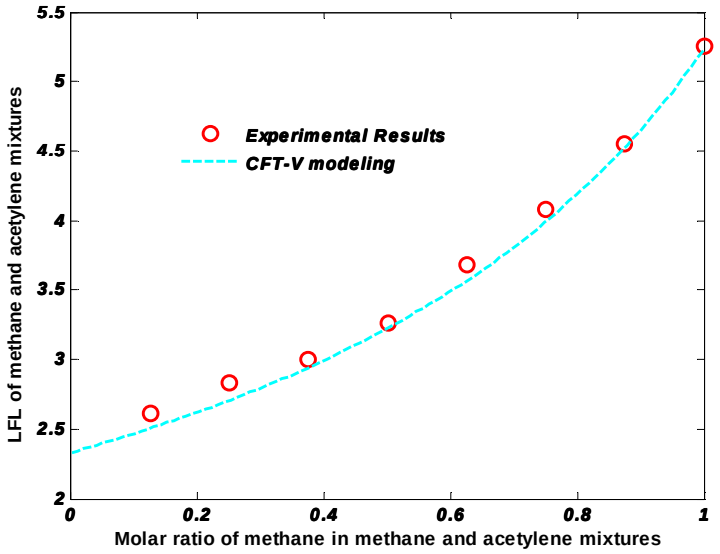


Fig. 5.5. Estimation of LFLs of methane and acetylene mixtures using CFT-V modeling at standard conditions.

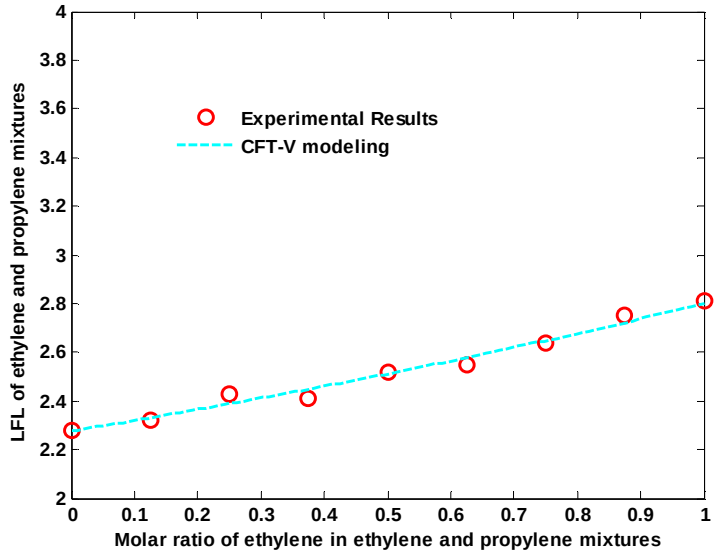


Fig. 5.6. Estimation of LFLs of ethylene and propylene mixtures using CFT-V modeling at standard conditions.

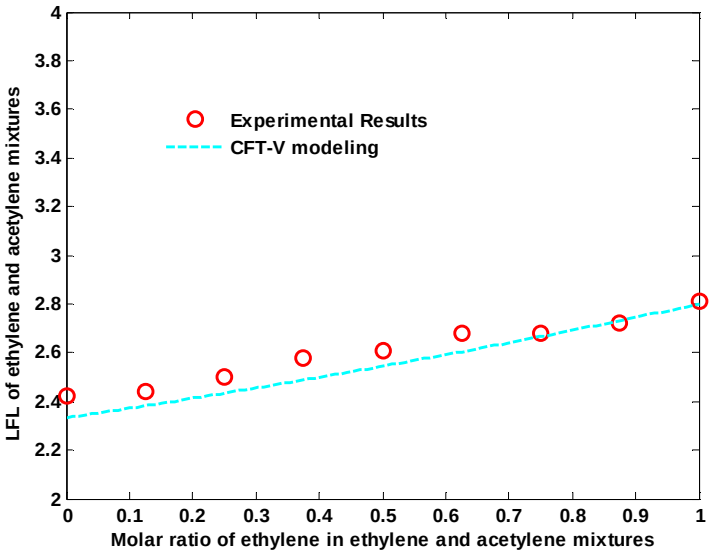


Fig. 5.7. Estimation of LFLs of ethylene and acetylene mixtures using CFT-V modeling at standard conditions.

Figure 5.8 - 5.12 show the comparisons of predicted LFLs using CFT-V modeling with those without considering heat losses for the binary hydrocarbon mixtures of methane and n-butane, methane and ethylene, methane and acetylene, ethylene and propylene, ethylene and acetylene, respectively, where the same calculated flame temperatures for each hydrocarbon mixture with/without heat losses were assumed [Table 5.5]. All the figures indicate that heat losses could considerably affect the lower flammability estimation based on the experimental configuration. Theoretically, if there is no heat loss from the reaction vessel, lower energy will be needed to activate the unburned fuel/air mixture for the continuous reaction taking place, which means a less fuel molar fraction can meet the requirement of flame propagation; therefore, the LFLs of the fuel/mixtures decrease accordingly.

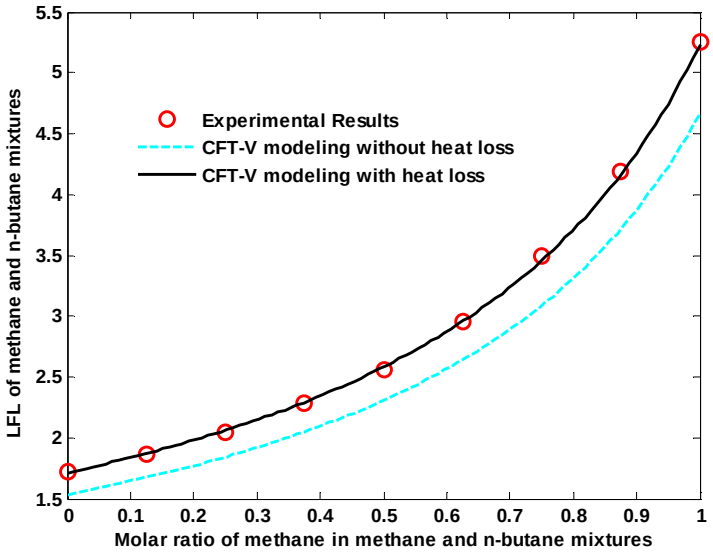


Fig. 5.8. LFLs of methane and n-butane mixtures using CFT-V modeling with/without consideration of heat loss at standard conditions.

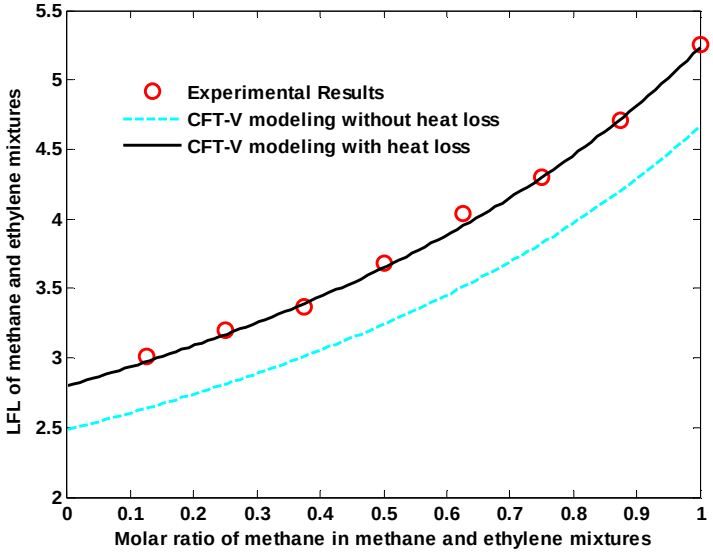


Fig. 5.9. LFLs of methane and ethylene mixtures using CFT-V modeling with/without consideration of heat loss at standard conditions.

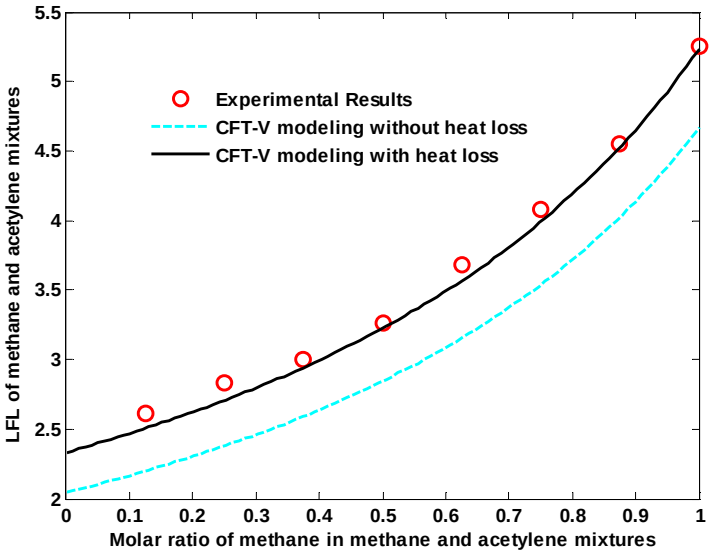


Fig. 5.10. LFLs of methane and acetylene mixtures using CFT-V modeling with/without consideration of heat loss at standard conditions.

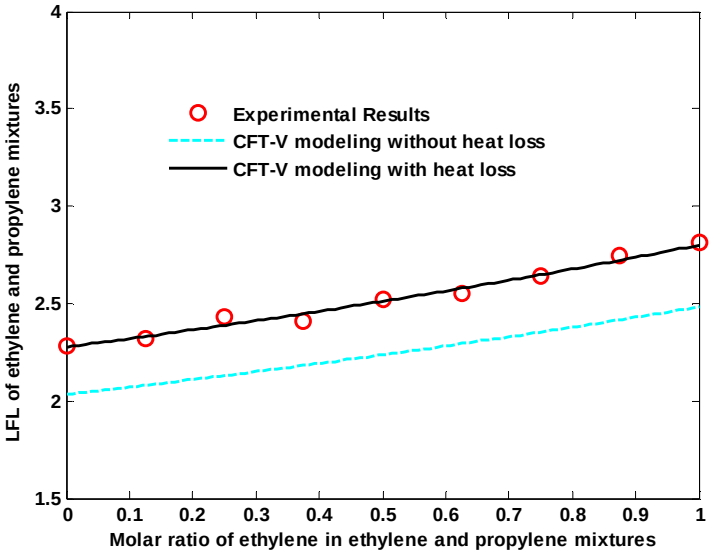


Fig. 5.11. LFLs of ethylene and propylene mixtures using CFT-V modeling with/without consideration of heat loss at standard conditions.

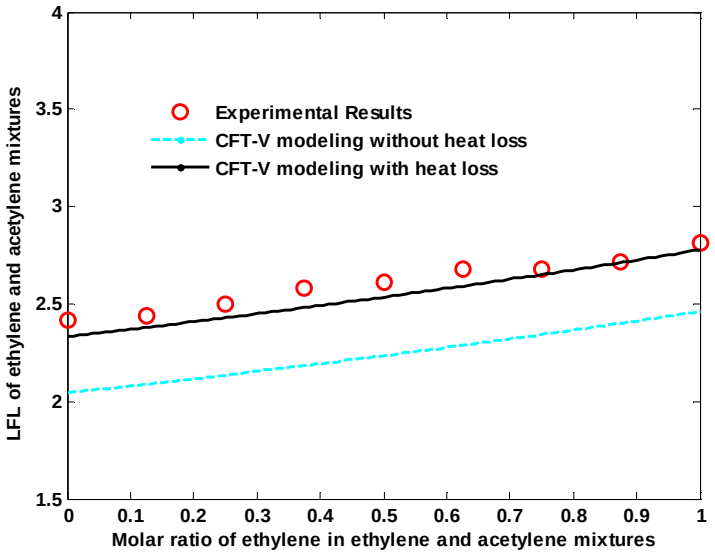


Fig. 5.12. LFLs of ethylene and acetylene mixtures using CFT-V modeling with/without consideration of heat loss at standard conditions.

Figure 5.13 - 5,17 present the predicted lower flammability limits for binary hydrocarbon mixtures with the combinations of methane and n-butane, methane and ethylene, methane and acetylene, ethylene and propylene, and ethylene and acetylene, respectively, by using different estimation methods to determine the flame temperature of fuel/air mixtures (e.g., constant flame temperatures 1200 K and 1600 K; linear flame temperature Eq. (59); method using CFT-V modeling Eq. (55)) Based on the governing equation (Eq. (39)), the final flame temperature for a fuel/air mixture is a key parameter that impacts the estimation of flammability limits using CFT-V modeling.

$$T_{F,mix} = x \cdot T_{F,1} + (1-x) \cdot T_{F,2} \tag{59}$$

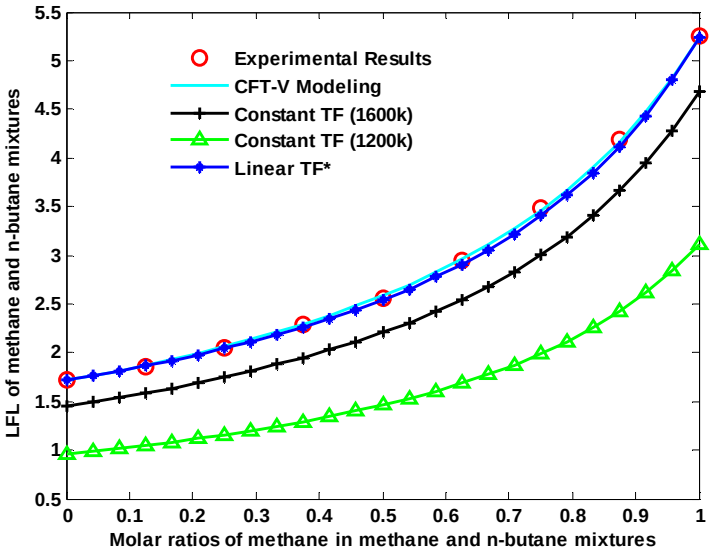


Fig. 5.13. LFLs of methane and n-butane mixtures using CFT-V modeling with different flame temperature estimation methods at standard conditions.

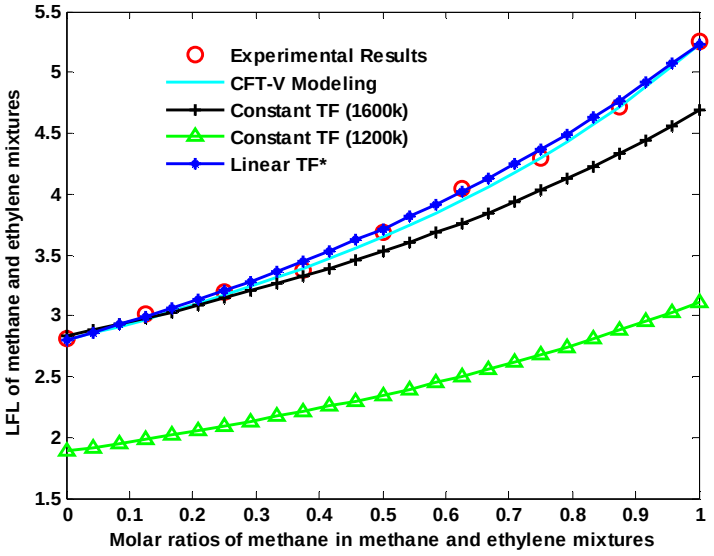


Fig. 5.14. LFLs of methane and ethylene mixtures using CFT-V modeling with different flame temperature estimation methods at standard conditions.

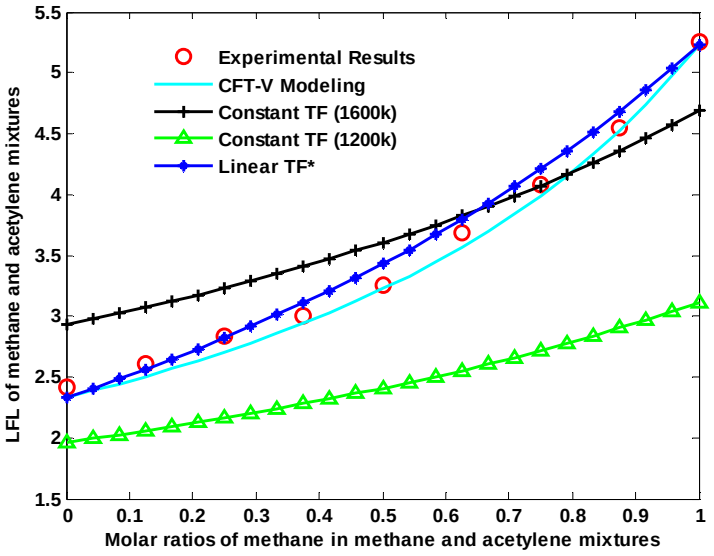


Fig. 5.15. LFLs of methane and acetylene mixtures using CFT-V modeling with different flame temperature estimation methods at standard conditions.

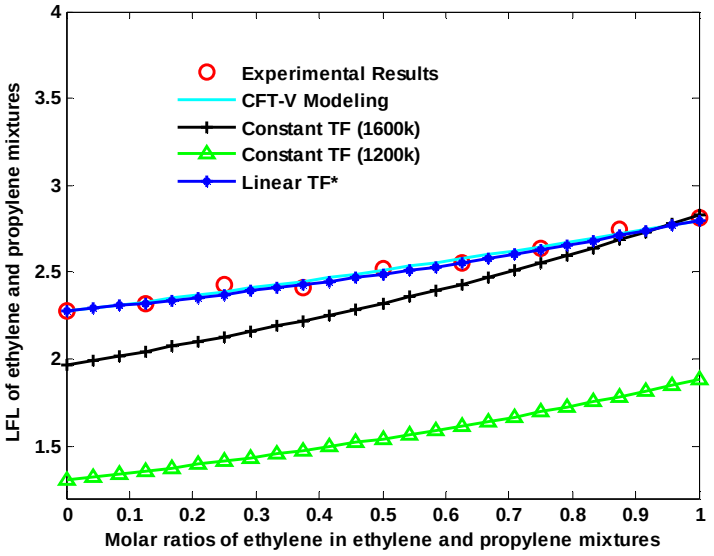


Fig. 5.16. LFLs of ethylene and propylene mixtures using CFT-V modeling with different flame temperature estimation methods at standard conditions.

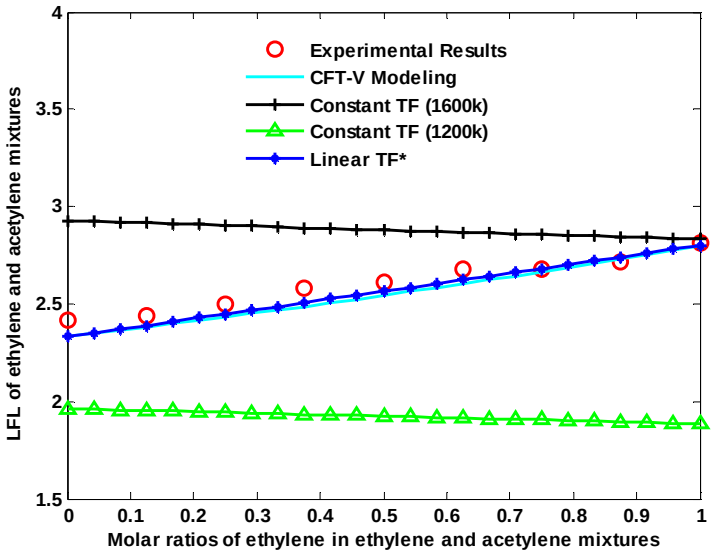


Fig. 5.17. LFLs of ethylene and acetylene mixtures using CFT-V modeling with different flame temperature estimation methods at standard conditions.

Figure 5.18 - 5.22 show the comparisons of predicted lower flammability limits (methane and n-butane, methane and ethylene, methane and acetylene, ethylene and propylene, ethylene and acetylene) using CFT-V modeling and CAFT modeling (using flame temperature data from Table 5.5).

The application assumptions for CAFT modeling include constant pressure, constant enthalpy, and no heat loss to environment, which turns out to be an approximate simplification in this research. Because under experimental conditions in this research, the closed reaction vessel cannot ensure constant pressure during the reaction, the carbon steel reaction vessel wall cannot guarantee the ideal heat insulation as well.

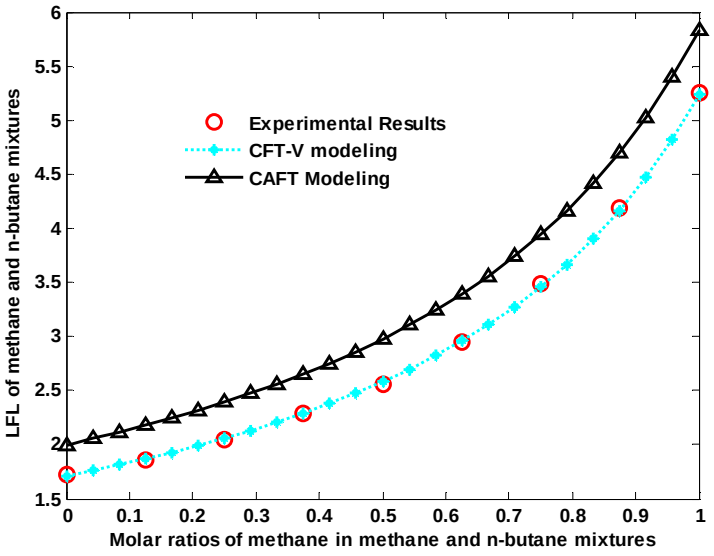


Fig. 5.18. Comparison of the predicted LFLs of methane and n-butane mixtures using CFT-V modeling and CAFT modeling at standard conditions.

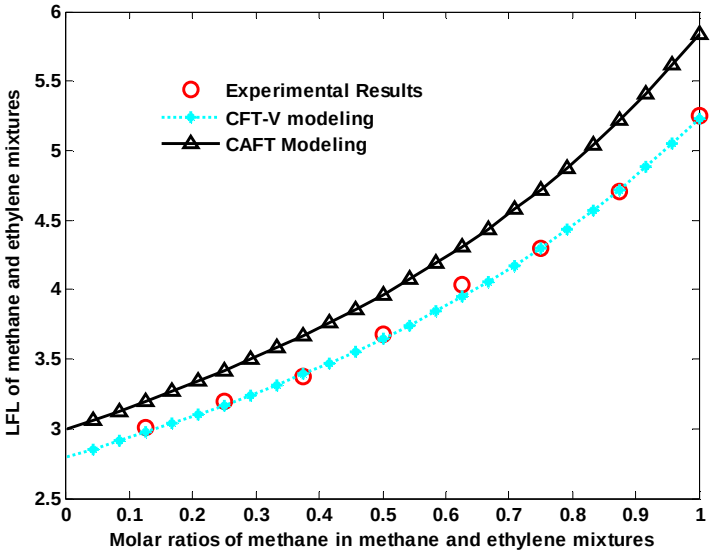


Fig. 5.19. Comparison of the predicted LFLs of methane and ethylene mixtures using CFT-V modeling and CAFT modeling at standard conditions.

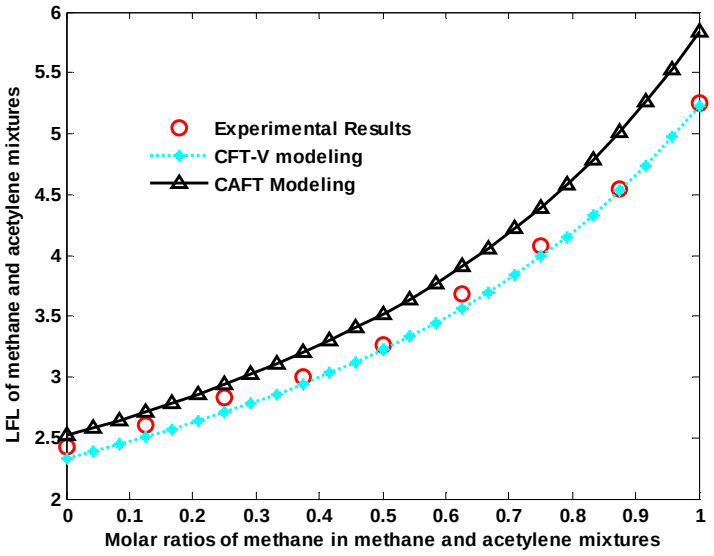


Fig. 5.20. Comparison of the predicted LFLs of methane and acetylene mixtures using CFT-V modeling and CAFT modeling at standard conditions.

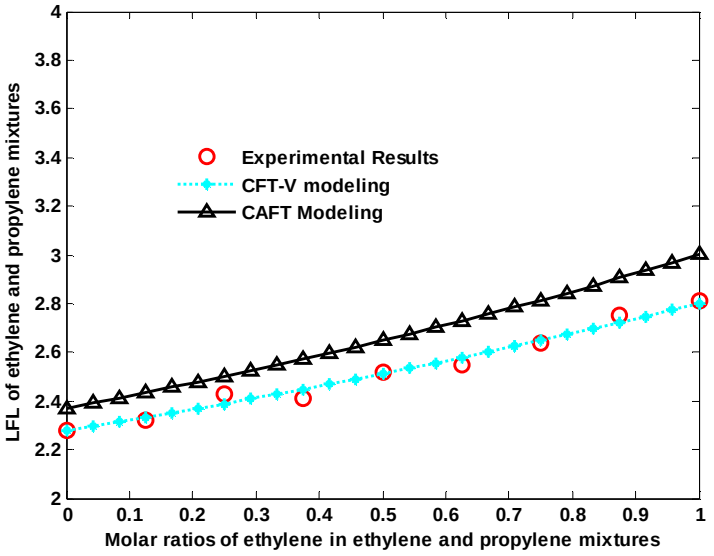


Fig. 5.21. Comparison of the predicted LFLs of ethylene and propylene mixtures using CFT-V modeling and CAFT modeling at standard conditions.

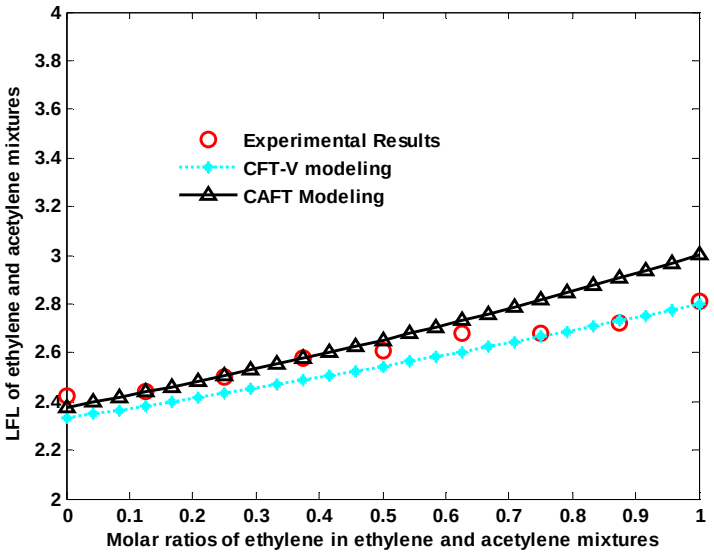


Fig. 5.22. Comparison of the predicted LFLs of ethylene and acetylene mixtures using CFT-V modeling and CAFT modeling at standard conditions.

### 5.4 Conclusions and Discussions

CFT-V modeling construction and application are another objective of this research. Similar to experimental observations of flammability limits for binary hydrocarbon mixtures (methane and n-butane, methane and ethylene, methane and acetylene, ethylene and propylene, ethylene and acetylene), the modeling predictions were conducted using CFT-V modeling for these fuel mixture flammability limit estimations.

In this modeling part, comprehensive energy conservation was considered, where heat generation is from the combustion of fuel/air mixtures in the reaction vessel; heat loss includes natural convection through the reaction vessel outside surface and heat absorption into the reaction vessel body. Because heat loss is related to the apparatus configuration, the construction of the CFT-V model was completely based on the

reaction vessel. The reaction vessel has a cylindrical geometry with I.D. 10.22 cm, compared with the reactors with spherical shape and central ignition, the cylindrical vessel is easy to lose heat from combusting fuel/air mixture. Moreover, the reaction vessel body is made from highly thermal-conductive carbon steel. Therefore, heat loss in this experimental configuration cannot be ignored.

Application of CFT-V modeling is a four-step procedure: firstly, measuring the lower flammability limits of fuel; secondly, determining the flame temperature of these pure fuels based on comprehensive energy conservation; next, estimating the flame temperatures of the fuel mixture; and lastly, reusing energy conservation again, and calculating the lower flammability limits of the fuel mixtures. Because the flame temperatures for pure fuels are dependent on the experimental measurements (concentrations of flammability limits), and the flammability limit is a function of the experimental apparatus shape and size, the application of CFT-V modeling is a case-dependent operation.

Using a proper way to quantify the flame temperatures of the hydrocarbon mixtures is critically significant for accurate application of CFT-V modeling. Previous research on adiabatic flame temperature indicates that the adiabatic flame temperature is dependent on the combusting fuel. Different fuels at their lower flammability limits produce different adiabatic flame temperatures. The principle fits the CFT-V modeling as well.

The predictions from the CAFT modeling exhibit certain gaps with experimental measurements, where the generally-used CAFT modeling is only roughly applicable.

However, CFT-V represents a case-specified modeling, and estimations of flammability limits using this model are more accurate and applicable than CAFT modeling. However, based on the energy conservation expression, CFT-V modeling can be simplified to no heat loss if the reactor quenching effect is extremely small. Specifically, when the total mole changes in chemical reactions can be neglected and the quenching effect is small, CFT-V modeling can be simplified to CAFT modeling.

# CHAPTER VI

# CONCLUSIONS AND FUTURE STUDIES

## 6.1. Conclusions from This Research

In this research, two different ways were conducted to estimate the flammability limits of binary hydrocarbon mixtures: (i) Experimental measurement using an innovative detection, thermal criterion, and (ii) Modeling prediction by CFT-V modeling, which is an extended application of CAFT modeling at constant volume.

Five typical hydrocarbons were selected as representatives of the hydrocarbon family consisting of two saturated hydrocarbons (methane and n-butane), two double-bond hydrocarbons (ethylene and propylene), and one triple-bond hydrocarbon (acetylene). The representative binary hydrocarbon mixtures include methane and n-butane, methane and ethylene, methane and acetylene, ethylene and propylene, and ethylene and acetylene. The lower and upper flammability limits of these combinations were measured in the experimental part. For modeling estimation, only the lower flammability limits of these combinations were predicted.

Based on the experimental measurements, the lower flammability limits of the above binary hydrocarbon combinations were fit by Le Chatelier's Law very well; while for the cases of the upper flammability limits, the experimental observations for those mixtures that contain unsaturated hydrocarbons could not be fit by Le Chatelier's Law. If the fuel mixtures contain two saturated hydrocarbons, however, the experimentally measured data can be fit by Le Chatelier's Law. For accurate determination of the upper

flammability limits, those data which could not be fit by Le Chatelier's Law were numerically analyzed, specifically, to be fit by the modification of Le Chatelier's Law. The modification method is to power the fuel percentage concentrations using the maximum R-square value. Meanwhile, the ratios of experimentally measured flammability limit to stoichiometric concentration were quantitatively characterized with fuel percentage concentration, in which the ratio of lower flammability limit to stoichiometric concentration are linearly related to the fuel percentage concentration, while the ratios of upper flammability limit to stoichiometric concentration are quadratically related to the fuel percentage concentration.

CFT-V modeling methodology is based on the comprehensive consideration of energy balance, in which the heat generation by fuel combustion equals the heat loss plus holding energy in the reaction vessel heating reaction products. Because heat loss is related to the fuel combustion chamber configuration, CFT-V is a case-specified modeling, by which for different experimental configurations, the modeling predictions vary even with the same fuels and at the same experimental conditions. In this experimental configuration, heat loss to the environment could not be neglected. By using the measured lower flammability limits of the pure hydrocarbons in the experiment part, the combustion energy can be calculated when the chemical reaction has completed. The heat quota for the heating reaction products is the difference between the total energy production minus heat losses, therefore the flame temperature for each pure hydrocarbon at the concentration of the lower flammability limits can be estimated. Then, the flame temperatures for fuel mixtures were obtained using the

derived equation in this research. Finally, reusing the energy conservation equation, we can calculate the lower flammability limits for binary hydrocarbon mixtures.

**6.2 Future Studies**

This research on flammability limit estimation was focused on the standard conditions, but flammability data at nonstandard conditions (different temperatures and pressures, varied oxygen concentrations, or diluent impact of inert gases) are extremely sought after for a variety of industrial operations. The modification of Le Chatelier's Law was not a general result because the experimental data are only based on five selected hydrocarbons. In the future, more research work will be performed as follows:

- Continuing experimental measurements to estimate the lower and upper flammability limits for more binary hydrocarbon mixtures at standard conditions.
- Use of more experimentally measured data for data analysis. Finding whether there exists a general modification method for Le Chatelier's Law.
- Extend the binary hydrocarbon mixture system to multiple mixture systems. Measure the flammability limits and perform numerical analysis similar to that used for the binary hydrocarbon mixture system.
- Quantitatively characterize the effects from varied oxygen concentrations or inert gases dilutions.
- If modifications of experimental apparatus are available (e.g., additional heater, or design to change pressure), the flammability limit estimation for hydrocarbon mixtures will be conducted at non-standard conditions.

## REFERENCES

[1] G.D. De Smedt, D. De Corte, R. Notele, J. Berghmans, Comparison of two standard test methods for determining explosion limits of gases at atmospheric conditions, Journal of Hazardous Materials, A70 (1999) 105-113.

[2] M.G. Zabetakis, J. K. Richmond, The determination and graphic presentation of the limits of flammability of complex hydrocarbon fuels at low temperature and pressure, 4th symp. (internat.) on combustion, Williams & Wilkins Co., Baltimore, Md., (1953) 121-126.

[3] J. Bond, Sources of ignition: flammability characteristics of chemicals and products, Butterworth-Heinemann Ltd, Oxford, (1991) 7-10.

[4] M.G. Zabetakis, Flammability characteristics of combustible gases and vapors, Bulletin 627, Bureau of Mines, Pittsburgh (1965).

[5] M.G. Zabetakis, G.S. Scott, G.W. Jones, Limits of flammability of paraffin hydrocarbons in air, Ind. and Eng Chem. 43 (1951) 2120-2124.

[6] J.M. Kuchta, Investigation of fire and explosion accidents in the chemical, mining, and fuel-related industrial—A manual, Bulletin 680, Bureau of Mines, Pittsburgh (1985).

[7] M.G. Zabetakis, S. Lambiris, G.S. Scott, Flame temperature of limit mixtures, 7th Symposium on Combustion, Butterworths, London, (1959).

[8] C.M. Shu, P.J. Wen, R.H. Chang, Investigations on flammability models and zones for o-xylene under various initial pressure, temperatures and oxygen concentrations. Thermochimica Acta, (2002) 371-392.

[9] V. Babrauskas, Chapter 4: Ignition of gases and vapors. Ignition Handbook, Fire Science Publishers. Fire Science and Technology Inc. Issaquah, USA (2003).

[10] G.A. Melhem, A detailed method for estimating mixture flammability limits using chemical equilibrium, Process Safety Progress, 16 (1997) 203-218.

[11] S. Besnard, Full flammability test of gases and gas mixtures in air. CERN Report, (1996).

[12] L.G. Britton, Two hundred years of flammable limits, Process Safety Progress, 21(1) (2002) 1-11.

[13] H.F. Coward, G.W. Jones, Limits of flammability of gases and vapors, Bulletin 503, Bureau of Mines, Washington D.C. (1952).

[14] A. Takahashi, Y. Urano, K. Tokuhashi, S. Kondo, Effect of vessel size and shape on experimental flammability limit of gases, Journal of Hazardous Materials, A 105 (2003) 27-37.

[15] P.G. Guest, V.W. Sikora, B. Lewis, Static electricity in hospital operating suites: direct and related hazards and pertinent remedies. BuMines Rept. of Inv. 4833 (1952).

[16] V. Dolah, W. Robert, M.G. Zabetakis, D.S. Burgess, G.S. Scott, Review of fire and explosion hazards of flight vehicle combustibles, BuMine Inf. Circ. 8137 (1962).

[17] F. Clowes, Detection and estimation of inflammable gas and vapor in air, J. Soc. Arts 41 (1896) p307.

[18] P. Eitner, Untersuchungen uber die Explosionsgrenzen brembarer Gase und Dampe, Jour. Gasbel.,Jahrg. 45 (1902) p22.

[19] A.G. White, Limits for the propagation of flame in inflammable gas-air mixtures, J. Chem. Soc. 125 (1924) 2387-2396.

[20] R.G. Abdel-Gayed, D. Bradley, M. McMahon, Turbulent flame propagation in premixed gases: theory and experiment, 17$^{th}$ Symp. (Intl.) on Combustion, the Combustion Institute, Pittsburgh (1978) 245-254.

[21] P.M. Boston, Flame initiation in lean, quiescent and turbulent mixtures with various igniters, 20$^{th}$ Symp. (Intl.) on Combustion, the Combustion Institute, Pittsburgh (1984) 141-149.

[22] D.S. Burgess, A.L. Furno, J.M. Kuchta, K.E. Mura, Flammability of mixed gases, Bureau of Mines, Report of Investigations RI 8709 (1982).

[23] K.L. Cashdollar, I.A. Zlochower, G.M. Green, R.A. Thomas, M. Hertzberg, Flammability of methane, propane, and hydrogen gases, Journal of Loss Prevention in the Process Industries, 13 (2000) 327-340.

[24] Y. Ju, H. Guo, K. Maruta, Determination of burning velocity and flammability limit of methane/air mixture using counterflow flames, Jpn. J. Appl. Phys. 38 (1999) 961-967.

[25] ASTM, Standard test method for concentration limits of flammability of chemicals, ASTM E 681-01 (2001).

[26] ASTM, Standard test methods for limiting oxygen (oxidant) concentration in gases and vapors, ASTM E 2079-01 (2001).

[27] ASTM, Standard practice for determining limits of flammability of chemicals at elevated temperature and pressure, ASTM E 918-83 (1999).

[28] V. Schroder, M. Molnarne, Flammability of gas mixtures Part 1: fire potential, Journal of Hazardous Materials, A121 (2005) 37-44.

[29] A.A. Shimy, Calculating flammability characteristics of combustible gases and vapors, Fire Technology, 6 (1970) 135-139.

[30] A. Edgerton, J. Powling, The limits of flame propagation at atmospheric pressure II: the influence of changes in the physical properties, Proc. Royal Society, vol. 193A (1948) 190-209.

[31] D.R. Stull, Fundamentals of fire and explosion, AIChE monograph series, vol. 73, No.10, American Institute of Chemical Engineers, (1977).

[32] J. G. Hansel, J. W. Mitchell, H. C. Klotz, Predicting and controlling flammability of multiple inert mixtures, Air Products and Chemicals, Inc. Prepared for Presentation at AIChE 25th Loss Prevention Symposium, Pittsburgh, 18-21 August (1991).

[33] G.A. Melhem, A detailed method for the estimation of mixture flammability limits using chemical equilibrium, AIChE 31st Loss Prevention Symposium, Houston, 9-13 March (1997).

[34] Y.N. Shebeko, W. Fan, I.A. Bolodian, V.Y. Navzenya, An analytical evaluation of flammability limits of gaseous mixtures of combustible-oxidizer-diluent, Fire Safety J. 37 (2002) 549-568.

[35] C.V. Mashuga, Determination of the combustion behavior for pure components and mixtures using a 20 L sphere, Chemical Engineering, Ph. D. dissertation, Michigan Technological University, Michigan, 1999.

[36] C.V. Mashuga, D.A. Crowl, Flammability zone prediction using calculated adiabatic flame temperature, Process Safety Prog. 18 (1999) 127-134.

[37] M. Vidal, W. Wong, W. J. Rogers, M.S. Mannan, Evaluation of lower flammability limits of fuel-air-diluent mixtures using calculated adiabatic flame temperature, Journal of Hazardous Materials, 130 (2006) 21-27.

[38] S.W. Benson, J.H. Buss, Additivity rules for the estimation of molecular properties. Thermodynamic Properties, the Journal of Chemical Physics, 29(3) (1958) 546-572.

[39] M.R Reid, J.M. Prausnitz, B.E. Polling, The properties of gases and liquids, New York: Hill, (1987).

[40] T.A. Albahri, Flammability characteristics of pure hydrocarbons, Chemical Engineering Science, 58 (2003) 3629-3641.

[41] S. Kondo, Y. Urano, K. Tokuhashi, A. Takahashi, and K. Tanaka, Prediction of flammability of gases by using F-Number analysis, Journal of Hazardous Materials, A82 (2001) 113-128.

[42] American Society of Heating, Refrigerating and Air-conditioning Engineers, Number designation of safety classification of refrigerants, proposed addendum to ANSI/ASHRAE 34-1997, 3rd Public Review Draft, ASHRAE, Atlanta, GA, (1999).

[43] S. Kondo, K. Takizawa, A. Takahashi, K. Tokuhashi, Extended Le Chatelier's formula for carbon dioxide dilution effect on flammability limits, Journal of Hazardous Materials, A138, (2006) 1-8.

[44] C.V. Mashuga, D.A. Crowl, Derivation of Le Chatelier's mixing rule for flammability limits, Process Safety Progress, 19 (2) (2000) 112-117.

[45] G.W. Jones, E.S. Harris, W.E. Miller, Explosive properties of acetone-air mixtures, U.S. Bureau of Mines, Technical Paper 544, (1933).

[46] W.K. Wong, Measurement of flammability in a closed cylindrical vessel with thermal criterion, Ph. D. dissertation, Department of Chemical Engineering, Texas A&M University, (2006).

[47] I. Wierzba, G.A. Karim, H. Cheng, The flammability of rich gaseous fuel mixtures including those containing propane in air, Journal of Hazardous Materials, 20 (1988) 303-312.

[48] C.E. Baukal, R.E. Schhartz, Chapter 3: Heat transfer, the John Zink combustion handbook, John Zink Company, LLC, Tulsa, Oklahoma (2001).

[49] L.S. Marks, Mechanical engineers handbooks, New York: McGraw-Hill Book Company, Inc. (1941).

[50] V. Babrauskas, Chapter 15: Tables (Pure chemical substances). Ignition handbook, Fire Science Publishers. Fire Science and Technology Inc. Issaquah, USA (2003).

[51] M. Vidal, W. Wong, W.J. Rogers, M.S. Mannan, Evaluation of lower flammability limits of fuel-air-diluent mixtures using calculated adiabatic flame temperatures, Journal of Hazardous Materials, 130 (2006) 21-27.

# VITA


Name: Fuman Zhao

Address: May Kay O'Connor Process Safety Center, Division
Artie McFerrin Department of Chemical Engineering
Texas A&M University
College Station, TX 77843-3136

E-mail Address: zhaofuman@neo.tamu.edu


Education: B.S., Chemical Engineering, 1998
University of Tianjin, China

M.S. Environmental Engineering, 2006
Texas A&M University

M.S. Chemical Engineering, 2008
Texas A&M University